

On simulating shoreline evolution using a hybrid 2D/one-line model

Avidesh Seenath

Faculty of Engineering, Environment and Computing, Coventry University, CV1 2LT, United Kingdom

ARTICLE INFO

Keywords:

Shoreline evolution modelling
One-line theory
Coastal geomorphology
Boundary conditions
Sandy coasts

ABSTRACT

Hybrid 2D/one-line shoreline models are becoming increasingly applied over the mesoscale (10^1 – 10^2 years; 10^1 – 10^2 km) to inform coastal management. These models typically apply the one-line theory to simulate changes in shoreline morphology based on littoral drift gradients calculated from a 2DH coupled wave, flow, and sediment transport model. However, the key boundary conditions needed to effectively apply hybrid 2D/one-line models and their applicability beyond simple planform morphologies are uncertain, which can potentially comprise coastal management decisions. To address these uncertainties, an extensive numerical modelling campaign is carried out to both assess the sensitivity and calibrate an advanced hybrid 2D/one-line model (MIKE21) against six variables in three different sandy coastal system morphologies: (a) a simple planform morphology with a gentle sloping profile, (b) a simple planform morphology with a steep sloping profile, and (c) a complex planform morphology. The six variables considered include nearshore discretisation, bathymetry, bed friction, sand grain diameter, sand porosity, sediment grading, and the weir coefficient of hard defence structures. Five key conclusions are derived from the sensitivity testing and calibration results. *First*, the optimal boundary conditions for modelling shoreline evolution vary according to coastal geomorphology and processes. *Second*, specifying boundary conditions within physically realistic ranges does not guarantee reliable shoreline evolution predictions. *Third*, nearshore discretisation should be treated as a typical calibration parameter as (a) the finest discretisation does not guarantee the most accurate predictions, and (b) defining a discretisation based on process length scales also does not guarantee reliable predictions. *Fourth*, hybrid 2D/one-line models are not valid for application in complex planform morphologies plausibly because of the one-line theory assumption of a spatially invariable closure depth. *Fifth*, hybrid 2D/one-line models have limited applicability in simple planform morphologies where the active beach profile is subject to direct human modification, plausibly due to the one-line theory assumption of a constant time-averaged coastal profile form. These findings provide key theoretical insights into the drivers of shoreline evolution in sandy coastal systems, which have practical implications for refining the continued application of shoreline evolution models.

1. Introduction

Modelling mesoscale shoreline evolution (10^1 – 10^2 years; 10^1 – 10^2 km) is becoming increasingly necessary for informing longer-term strategic management of sandy coastal systems, which continually adjust to subtle changes in external forcings (Table 1) (Payo et al., 2020). Coastal management is traditionally informed by shoreline evolution predictions from two-dimensional horizontal (2DH) or behaviour-oriented models (De Vriend et al., 1993; Hanson et al., 2003; Pontee, 2017). The shoreline, typically defined as the Mean High Water (MHW) line, is often considered a reliable proxy of overall coastal change. 2DH models, also referred to as process-driven models, simulate the physics of shoreline evolution, incorporating the temporal and spatial effects of various combinations of external forcings. However,

2DH models are limited to micro timescales (hours to years) because they cannot represent the vertical variation of undertow currents, the primary driving flux of cross-shore sediment transport that evolves the coastal profile (Franz et al., 2017). Consequently, the coastal profile gradually degenerates to an unrealistic shape in 2DH simulations longer than micro timescales (Kristensen et al., 2013; Franz et al., 2017). In contrast, behaviour-oriented models assume an equilibrium active coastal profile based on the one-line theory or the Bruun Rule. The active coastal profile extends from the beach berm to closure depth. The closure depth is widely regarded in coastal engineering as an empirical measure of the seaward limit of significant cross-shore sediment transport, which corresponds to the depth limit of significant wave action, in sandy coastal systems (Nicholls et al., 1999; Valiente et al., 2019). The one-line theory assumes the active coastal profile moves shore-normal

E-mail address: avidesh.seenath@coventry.ac.uk.

<https://doi.org/10.1016/j.coastaleng.2022.104216>

Received 27 March 2022; Received in revised form 29 July 2022; Accepted 10 September 2022

Available online 17 September 2022

0378-3839/© 2022 The Author. Published by Elsevier B.V. This is an open access article under the CC BY license (<http://creativecommons.org/licenses/by/4.0/>).

Table 1

External forcings associated with each established scale of shoreline evolution (adapted from [Stive et al., 2002](#)).

Scale	Natural forcing	Human forcing
Macro Space dimensions: ≥ 100 km Time dimensions: centuries to millennia	⇒ Sediment availability ⇒ Relative sea-level changes ⇒ Differential bottom changes ⇒ Geological setting ⇒ Long-term climate changes ⇒ Paleomorphology (inherited morphology)	⇒ Human-induced climate change ⇒ Major river regulation ⇒ Major coastal structures ⇒ Major reclamations and closure ⇒ Structural coastal (non)management
Meso Space dimensions: $\sim 10 - 100$ km Time dimensions: decades to centuries	⇒ Relative sea-level changes ⇒ Regional climate variations ⇒ Coastal inlet cycles ⇒ Sand waves ⇒ Extreme events	⇒ River regulation ⇒ Coastal structures ⇒ Reclamations and closures ⇒ Coastal (non) management ⇒ Natural resource extraction (subsidence)
Synoptic Space dimensions: $\sim 1 - 5$ km Time dimensions: years to decades	⇒ Wave climate variations ⇒ Surf zone bar cycles ⇒ Extreme events	⇒ Surf zone structures ⇒ Shore nourishments
Micro Space dimensions: ~ 10 m – 1 km Time dimensions: hours to years	⇒ Wave, tide, and surge conditions ⇒ Seasonal climate variations	

from littoral drift, whereas the Bruun Rule assumes the active coastal profile shifts upward and landward in response to sea-level rise ([Pel-nard-Considere, 1956](#); [Bruun, 1962](#)). The exclusion of the underlying physics in model calculations and the assumption of an equilibrium active coastal profile ensure a stable morphology update over meso timescales, but prevent behaviour-oriented models from simulating the combined effects of external forcings that drive shoreline evolution ([Pontee, 2017](#)). Also, an equilibrium active coastal profile implies shore-parallel contours (simple planform morphology), limiting the applicability of behaviour-oriented models in complex planform morphologies ([Hurst et al., 2015](#)). These morphologies are defined by non-parallel depth contours, characteristic of vulnerable sandy coastal systems in many Caribbean and Pacific small islands ([Mycioo and Donovan, 2017](#)), where shoreline evolution models are arguably most needed to inform coastal management.

The limitations of 2DH and behaviour-oriented models have inspired the development of hybrid 2D/one-line models for simulating mesoscale shoreline evolution ([Kaergaard and Fredsoe, 2013](#)). These models maintain the physics-driven approach of 2DH models but use the one-line theory assumptions to update the shoreface morphology ([Fig. 1](#)). Specifically, they simulate the physics of coastal sediment transport, incorporating the combined effects of external forcings and complex planform morphologies, and uniformly redistribute the derived littoral drift gradients over the active coastal profile. The active coastal profile moves shore-normal from a change in sediment balance, resulting in a change in shoreline position. Using the one-line theory assumptions to update the shoreface morphology prevents the breakdown of coastal profiles, allowing hybrid 2D/one-line models to simulate mesoscale shoreline evolution whilst maintaining the underlying

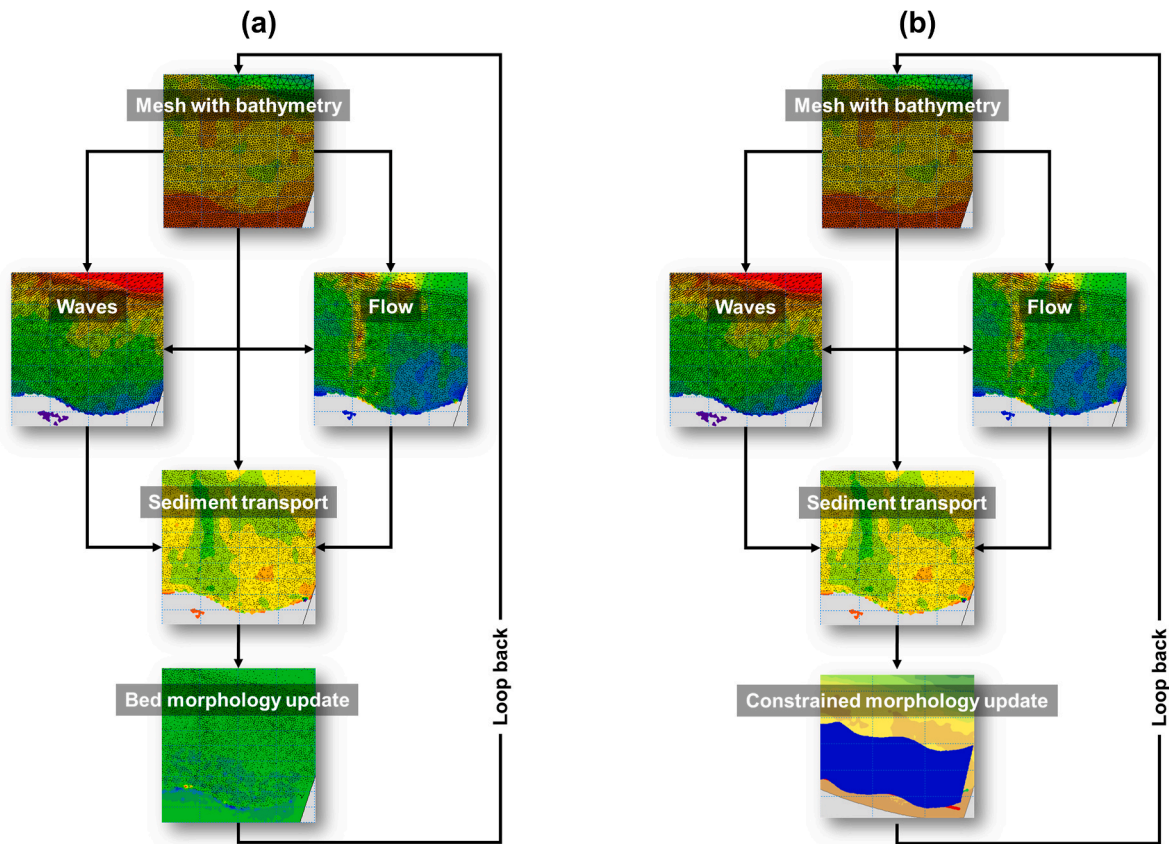


Fig. 1. Computational framework of 2DH (a) and hybrid 2D/one-line shoreline models (b). The main computational difference between both types of models is the shoreline morphology update. (a) shows that 2DH models update the morphology in the entire domain at each time-step. The change in morphology from one time-step updates the mesh bathymetry for the next time-step to continue the simulation in 2DH models. (b) shows that hybrid 2D/one-line models maintain the same principles as 2DH models, except constrain the morphology update within the limits of the active coastal profile.

physics. Although hybrid 2D/one-line models appear promising for enabling mesoscale shoreline evolution simulations, the applicability of these models beyond simple planform morphologies is not yet known, especially since these models apply the one-line theory in the shoreline morphology update, which assumes shore-parallel depth contours. Also, most applications of the hybrid 2D/one-line approach have been experimental for illustrating their proof of concept without extensive validation (e.g. Slott et al., 2010; Barkwith et al., 2014; Van Maanen et al., 2016; Payo et al., 2020). Therefore, the usefulness of this approach for simulating shoreline evolution across morphologies at scales relevant for informing coastal management remains uncertain.

Furthermore, the largest constraint in refining and applying shoreline evolution models is the availability of high-quality data to specify boundary conditions (Splinter et al., 2013; Reeve et al., 2019). Boundary conditions include nearshore bathymetry, coastal processes, and sediment properties, all of which influence sediment transport and shoreline morphology. There are no established guidelines on the appropriate resolution of boundary conditions data for modelling shoreline evolution. Instead, it is usually assumed that higher resolution data improve shoreline evolution predictions, but this assumption is never typically tested due to a global lack of high-resolution bathymetry and coastal processes data. Related studies use data either available, surveyed or extrapolated from past data without quantifying the effects on model predictions. There is also a tendency in related literature to accept default values of free parameters (e.g. friction) in shoreline evolution models that broadly characterise the coastal system of interest. Using model default values and limited, coarse, or extrapolated data to specify boundary conditions can generalise complex coastal processes and adversely affect shoreline evolution predictions (Le Cozannet et al., 2019; Cooper et al., 2020). As it stands, the optimal boundary conditions (types and data) for simulating shoreline evolution are not yet defined. In addition to shoreline evolution predictions, data scarcity also affects the design of appropriate coastal management schemes, especially in small island states of the Caribbean and Pacific (Mycio and Donovan, 2017; Rölfer et al., 2020). Identifying the optimal requirements for modelling shoreline evolution is important for being able to refine the intrinsic structure of shoreline evolution models to better support coastal management.

This paper aims to (a) assess the sensitivity of the hybrid 2D/one-line approach to key boundary conditions in sandy coastal systems; and (b) determine the validity and applicability of this approach in and beyond

simple planform morphologies. Anticipated outcomes will improve our understanding of the main controls on shoreline evolution in sandy coastal systems. This knowledge will have practical implications for refining the continued development and application of mesoscale-type shoreline evolution models to better support coastal management. Subsequent sections provide details of the test sites (Section 2), data and modelling approaches (Section 3), results (Section 4) and their wider implications (Section 5), and a summary of the key findings (Section 6).

2. Test sites

Three test sites are selected in locations with a contrasting coastal geomorphology and high-resolution bathymetry, tide, wind and wave climate data. These include a managed sandy coastal system in New York (Fig. 2), Puerto Rico (Fig. 3), and Southern California (Fig. 4), each described in subsequent paragraphs. Fig. 5 compares the coastal profile morphology in each test site.

The New York test site encompasses the Atlantic coastline of Long Beach Barrier Island and has a 12.5 km sandy shoreline that is managed by 43 groynes (Fig. 2a-b). The shoreline, which is defined herein as the MHW line, is concave in the east and west and generally straight elsewhere, except for deformations from accretion (erosion) updrift (downdrift) of groynes (Fig. 2b). The area is microtidal (mean tide range = 1.43 m) and has a simple planform morphology (Fig. 2c). The average coastal profile gently slopes and decreases monotonically cross-shore, mirroring the envelope of coastal profiles sampled every 15 m longshore from a 2014 Digital Elevation Model (DEM) (Fig. 5a).

The Puerto Rico test site is an almost 5 km sandy coastal stretch, located along the Atlantic coast of the island in San Juan (Fig. 3). The shoreline here has a cusped-cape shape, and is managed by breakwaters, seawalls, and groynes, and buffered by fringing reefs (Fig. 3b-c). The area is microtidal (mean tide range = 0.34 m) and has a complex planform morphology in response to the irregular spatial distribution of reef substrate (Fig. 3c). The average coastal profile is characterised by a steep upper beach and a gentle lower beach (Fig. 5b). However, the envelope of coastal profiles sampled every 15 m longshore from a 2014 DEM shows considerable cross-shore variability in the seafloor (Fig. 5b).

The Southern California test site is an 11 km sandy coastal stretch in Santa Monica, which is managed by eight groynes and two jetties (Fig. 4a-b). The area is microtidal (mean tide range = 1.14 m) and has a simple planform morphology (Fig. 4c). The average coastal profile is

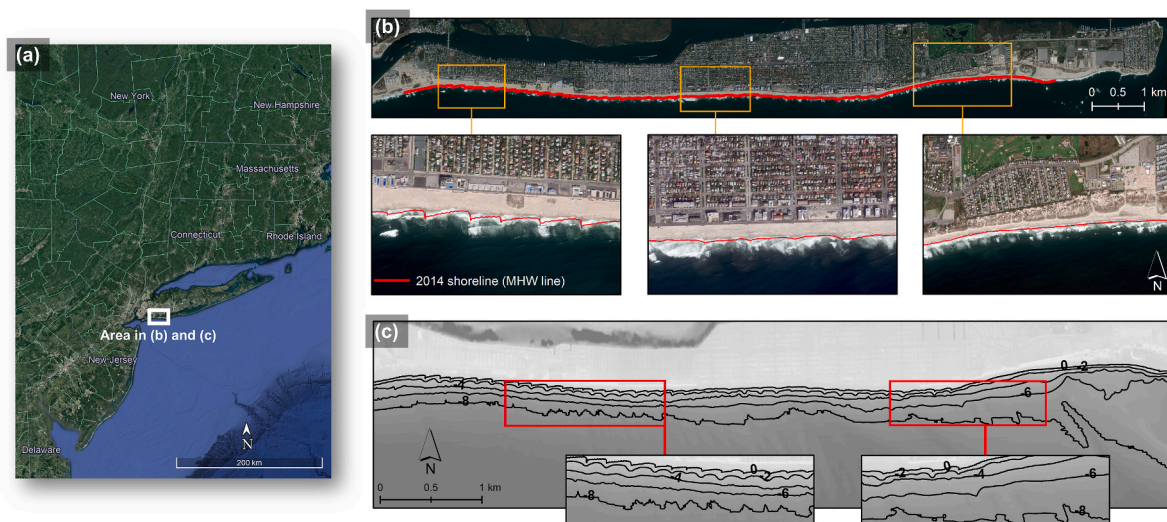


Fig. 2. Test site in New York. (a) Location along the United States East Coast. (b) 2012 GeoEye-1 image of the main site features: developed sandy coast, use of groynes for shoreline stabilisation, shoreline deformations around groynes, concave shoreline in the east and west, and a generally straight shoreline elsewhere. (c) Contour map illustrating shore-parallel depth contours in the nearshore. Credits: Google Earth (satellite image in a) and LAND INFO Worldwide Mapping (GeoEye-1 image in b).



Fig. 3. Test site in Puerto Rico. (a) Location in the Caribbean region. (b) 2013 orthophoto of the main site features: developed sandy coast, cusped shoreline, coral reefs, use of breakwaters and groynes for shoreline stabilisation, and use of seawalls for private property protection. (c) Contour map illustrating a complex planform morphology in the nearshore, defined by non-parallel depth contours. Credits: DigitalGlobe (satellite image in a) and USGS (orthophoto in b).

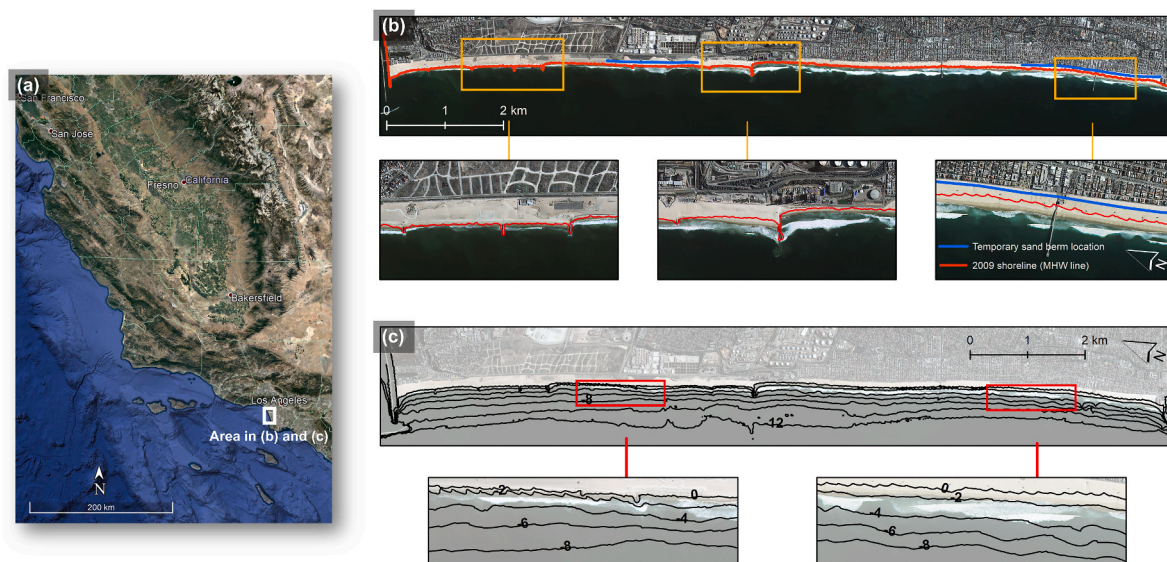


Fig. 4. Test site in Southern California. (a) Location along the United States West Coast. (b) 2013 KOMPSAT-2 image of the main site features: developed sandy coast, use of groynes and jetties for shoreline management, and a generally straight shoreline, with deformations mainly around groynes. (c) Contour map illustrating shore-parallel depth contours in the nearshore. Credits: DigitalGlobe (satellite image in a) and LAND INFO Worldwide Mapping (KOMPSAT-2 image in b).

steep and decreases monotonically seaward in slight contrast to the envelope of coastal profiles sampled every 15 m longshore from a 2009 DEM (Fig. 5c). The shoreline is mostly straight, with deformations mainly around groynes (Fig. 4b).

The contrasting coastal morphology of the above locations is ideal for addressing the aims of this paper, which seek to determine the key requirements and efficacy of the hybrid 2D/one-line approach for application in and beyond simple planform morphologies. The New

York and Southern California test site have a simple planform morphology compared to the Puerto Rico test site. However, the Southern California test site has a steep sloping coastal profile morphology relative to the New York test site.

Hereafter, the abbreviation NY is used for the New York test site, PR for the Puerto Rico test site, and SC for the Southern California test site.

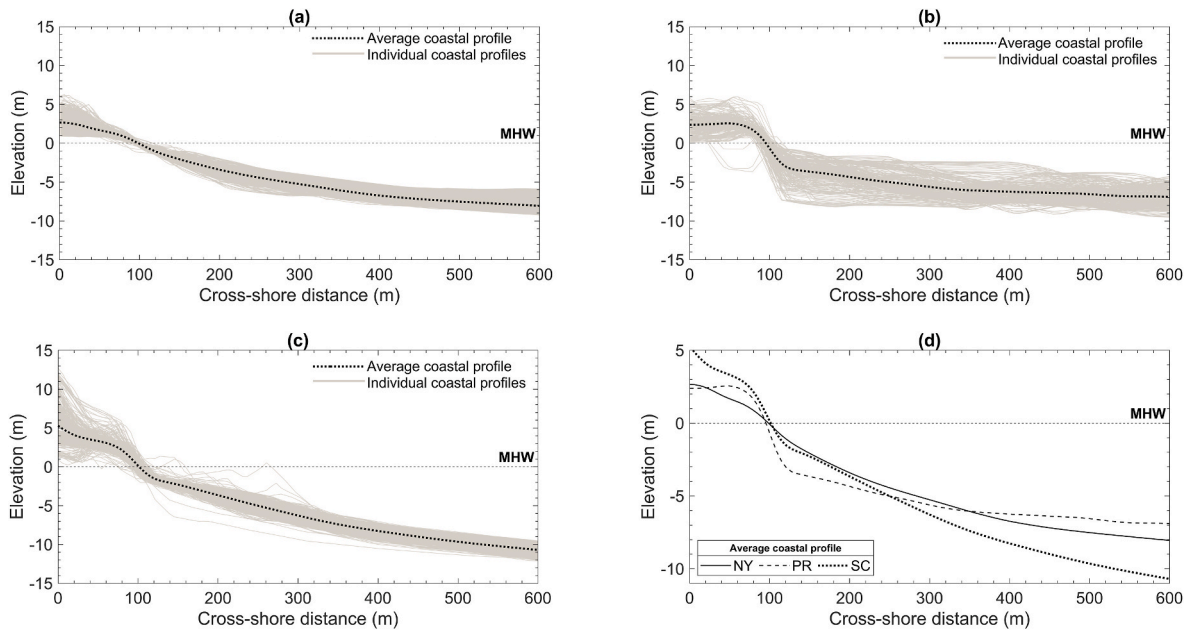


Fig. 5. Coastal profile morphology in each test site. (a), (b), and (c) show the coastal profile envelope and average coastal profile in the New York (NY), Puerto Rico (PR), and Southern California (SC) test site, respectively. The coastal profile envelope comprises individual coastal profiles sampled every 15 m longshore. The average coastal profile is the average of the individual coastal profiles. (d) compares the average coastal profile morphology in each test site.

3. Data and methods

3.1. Study periods and data

Considering the high-resolution DEMs and coastal processes data available (Table 2), model sensitivity testing and accuracy assessments are carried out from 2014 to 2016 in NY and PR, and from 2009 to 2011 in SC. These micro timescale periods are adequate to allow for (a) identifying the model inputs that cause the largest errors in shoreline evolution predictions, and (b) testing the validity of the hybrid 2D/one-line modelling approach. If a model fails to predict realistic shoreline change trends over micro timescales, the uncertainties introduced will propagate and generate unreliable predictions over meso timescales. Furthermore, the rates and patterns of shoreline change over meso timescales (i.e. primary timescale of concern in coastal management) are influenced by local drivers of coastal behaviour that operate at the micro timescale ($<10^1$ years), such as wave activity, tidal currents, supra-, inter-, and sub-tidal morphology, and sedimentology (Cattaneo and Steel, 2003; Cooper and Pilkey, 2004). Therefore, assessing the ability of a mesoscale shoreline evolution model to provide physically realistic predictions over micro timescales is a good first step towards identifying its fundamental limitations before applying it over meso timescales.

An initial and observed DEM, both vertically referenced to MHW (m) and horizontally referenced to WGS 84 (m), are obtained for each test site. The initial DEM contains topobathymetric data surveyed at the start of the study period, whereas the observed DEM contains topobathymetric data surveyed at the end of the study period. The shoreline position in each DEM is the zero-depth contour (i.e. the MHW line). The initial DEM and associated shoreline position provide the baseline for simulating shoreline evolution, whereas the shoreline position in the observed DEM is used as the benchmark for quantifying the accuracy of shoreline evolution predictions.

Table 2 lists the tide, wind, and wave climate data obtained for simulating shoreline evolution in each test site. All tide data are vertically referenced to MHW (m). All wind data include wind speed (m/s) and direction (deg), and all wave climate data include wave height (m), period (s), and direction (deg).

Data on the location and geometry of hard defences (e.g. groynes) are obtained from a geo-referenced GeoEye-1 image (0.5 m resolution) in NY, orthophoto in PR (0.1 m resolution), and KOMPSAT-2 image (1 m resolution) in SC. The elevation of the defences in each test site is derived from their initial DEM.

Table 2

Data obtained for model sensitivity testing in the New York (NY), Puerto Rico (PR), and Southern California (SC) test site.

Data	Time-period	Horizontal datum	Vertical datum	Units	Resolution	Source
Initial DEM	NY: 01-Jan-2014 PR: 01-Oct-2014 SC: 01-Jan-2009	WGS84	MHW	m	NY; PR: 3 m SC: 10 m	NY: NCEI (2017a) PR: NCEI (2019) SC: NCEI (2017b)
Observed DEM	NY: 01-Feb-2016 PR: 31-Mar-2016 SC: 02-Aug-2011				NY; PR: 3 m SC: 1 m	NY: NOAA (2017b) PR: NOAA (2019) SC: NOAA (2017a)
Tide	NY: 01-Jan-2014 – 01-Feb-2016 PR: 01-Oct-2014 – 31-Mar-2016 SC: 01-Jan-2009 – 02-Aug-2011	Not applicable			NY; PR; SC: 6 min	NY: NOAA (2017d) PR: NOAA (2017c) SC: NOAA (2017e)
Wind speed			Not applicable	m/s		NY: NDBC (2017a) PR: NDBC (2017b) SC: NDBC (2017c)
Wind direction				deg		
Wave height				m	NY; PR: 60 min SC: 30 min	
Wave direction				deg		
Wave period				s		

3.2. Model selection

Following an extensive review of the existing capabilities of shoreline evolution models (Table 3), MIKE21 Shoreline Morphology model, hereafter MIKE21, is selected to address the aims of this paper for two reasons. *First*, MIKE21 facilitates coupled 2DH wave, flow, and sediment transport simulations on a finite volume mesh over meso timescales. Such long-term simulations are possible because MIKE21 applies the one-line theory to constrain the shoreline morphology update, which prevent the erroneous degeneration of coastal profiles that restricts process-driven models to micro timescales. The use of a finite volume discretisation enables MIKE21 to consider the combined effects of various external forcings, such as wave climate, sea-level rise, and coastal defences, on littoral drift gradients over both simple (shore-parallel contours) and complex (non-parallel contours) planform morphologies.

The *second* reason for selecting MIKE21 is that it uses local coordinates for the shoreline morphology update. The use of local coordinates allows each point along a shoreline to evolve perpendicular to its orientation in contrast to fixed x,y coordinates, which enables MIKE21 to handle shorelines with curvature and undulations. Using fixed x,y coordinates to simulate shoreline evolution in areas with curvature and undulations tend to destabilise shoreline continuity solutions as multiple y coordinates share an x coordinate (Kaergaard and Fredsoe, 2013).

The ability to accommodate complex shoreline geometries and non-parallel depth contours in meso timescale coastal process simulations means that MIKE21 (a) offers the most advanced hybrid 2D/one-line modelling approach that is presently available as alternative hybrid models either possess one or none of these abilities, and (b) is the most appropriate hybrid model for handling the contrasting geomorphologies of the three test sites selected (Table 3). An important point to note here is that MIKE21 hybrid concept addresses key limitations of earlier versions of the hybrid 2D/one-line approach (see details in Kaergaard and Fredsoe (2013)). In theory, predictions from MIKE21, therefore,

represents the best outcomes we can get from applying the hybrid 2D/one-line approach to simulate shoreline evolution. It thus provides a sound basis for evaluating the hybrid 2D/one-line modelling approach that is becoming increasingly necessary for simulating mesoscale shoreline evolution.

3.3. Model description

MIKE21 combines a two-dimensional (2D) description of waves, hydrodynamics, and sediment transport with a one-line description of the shoreline position by coupling four modules, as illustrated in Fig. 6. It uses littoral drift gradients calculated from a coupled 2D wave, flow and sediment transport model to update the shoreface morphology in a one-line shoreline model. The littoral drift gradients are uniformly distributed over the active coastal profile, which moves seaward (landward) in response to sediment gain (loss) (Fig. 7). As this paper is essentially a sensitivity study of the hybrid 2D/one-line modelling approach, there is no modification of MIKE21 code. The following sections focus mainly on MIKE21 parameterisation and application in this study with little details on its computational structure as this model is a commercial software with extensive documentation on its setup (e.g. Seenath, 2021).

3.4. Mesh generation

The computational domain used to apply MIKE21 in each test site is defined in UTM coordinates with the following dimensions and specifications:

- (a) In NY, the domain is 12.5 km longshore and 2 km cross-shore, extending from ~2 m above MHW to a depth of 13 m below MHW, encompassing all land area at the site. The cross-shore dimensions of all computational domains generated in this study are determined based on observed coastal profile morphology and wave climate. In particular, the cross-shore

Table 3

Characteristics and capabilities of shoreline evolution models available (adapted from Pye et al. (2017)). Models that can be applied over meso timescales are highlighted in grey. 1DH is one-dimensional horizontal, and 2DH is two-dimensional horizontal. Y means capability included, and N means capability not included. C is cohesive, and NC is non-cohesive.

Model	Capability									
	Timescales ^a	Dimensions	Wave forcing	Wave-current interaction	Tidal forcing	Process sim. over non-parallel depth contours	Sea-level rise effects in shoreline evolution pred.	Sediment	Hard defences	Complex shorelines
Bruun Rule	Macro	2D	N	N	N	N	Y	NC	N	N
CEM	Macro	1DH, one-line	Y	N	N	N	N	C; NC	Y	Y
CoastalME	Meso	2DH, one-line	Y	N	N	N	N	C; NC	Y	Y
COVE	Macro	1DH, two-line	Y	N	N	N	N	C; NC	Y	Y
CSHORE	Micro	1DH, 2DH	Y	Y	N	N	N	NC	Y ^b	N
DELFT3D	Micro	2DH, 3D	Y	Y	Y	Y	Y	C; NC	Y	Y
GENESIS	Synoptic	1DH, one-line	Y	N	N	N	N	NC	Y	N
LITPACK	Meso	1DH, one-line	Y	Y	Y	N	N	NC	Y	N
MIKE21	Meso	2DH, one-line	Y	Y	Y	Y	N	NC	Y	Y
TELEMAC2D	Micro	2DH	Y	Y	Y	Y	Y	C; NC	Y	Y
UnaLinea	Meso	1DH, one-line	Y	N	N	N	N	C; NC	Y	Y
UNIBEST	Meso	1DH, one-line	Y	Y	Y	N	N	NC	Y	Y
XBeach	Micro	1DH, 2DH	Y	Y	Y	Y	Y	NC (sand)	Y	Y
XBeach-G	Micro	1DH	Y	Y	Y	Y	Y	NC (gravel)	Y	Y

^a See Table 1 for the definition of each timescale.

^b Low-crested stone structures only.

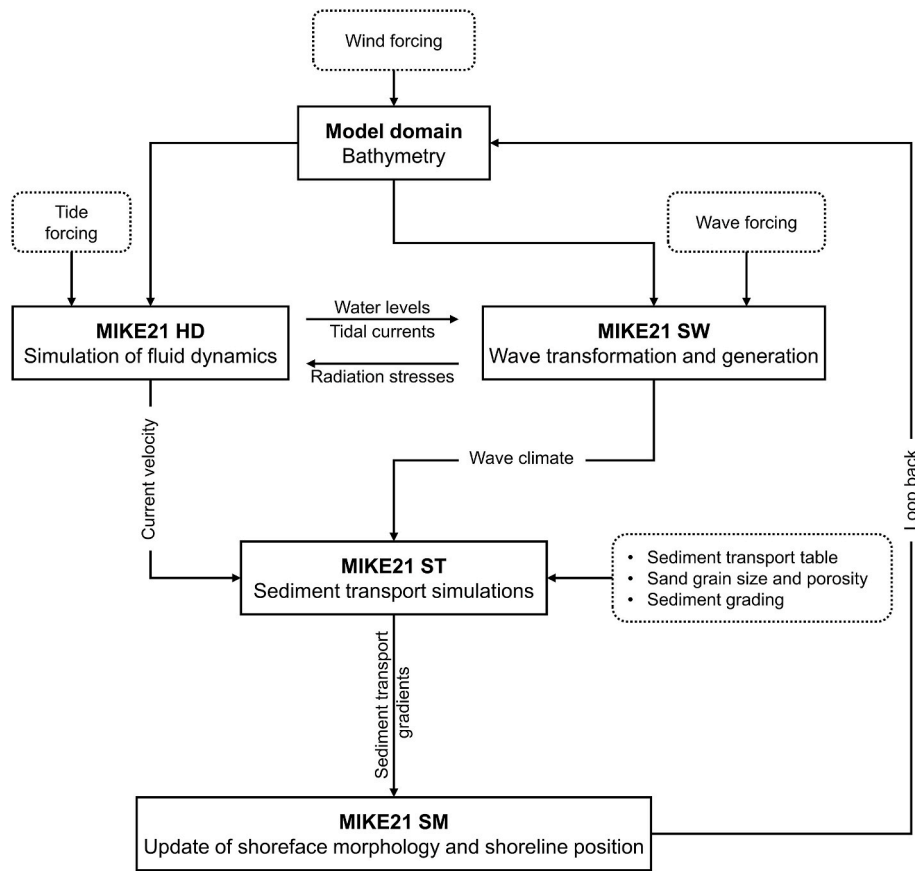


Fig. 6. MIKE21 computational framework for simulating shoreline evolution. HD is hydrodynamic, SW is spectral wave, ST is sediment transport, and SM is shoreline morphology.

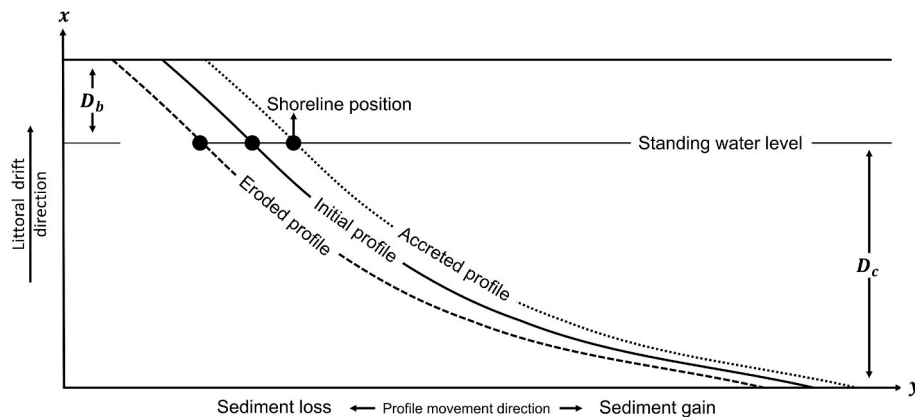


Fig. 7. One-line approach used for simulating shoreline evolution in hybrid 2D/one-line models, such as MIKE21. Shoreline change is a function of the shore-normal movement of the active coastal profile (beach berm - D_b - to closure depth - D_c). A gain (loss) in sediment shifts the active coastal profile seaward (landward).

dimensions extend beyond the closure depth (i.e. depth limit of significant wave action and cross-shore sediment transport) in order to facilitate realistic simulations of wave propagation. The mean wave height observed over the 2014–2016 study period at NY is 1.2 m (standard deviation = 0.69). Therefore, a 13 m depth boundary is sufficiently deep to facilitate wave approach to the shoreline since waves usually break at a depth equal to 1.2 times their height. In this study, the MHW line is treated as the shoreline position.

(b) In PY, the domain is 4 km longshore and 3 km cross-shore, extending from 5 m above MHW (400 m landward of the

shoreline) to 50 m below MHW, encompassing the full cross-shore extent of the fringing reef network. The sea boundary is particularly deep to allow wave propagation over the fringing reefs and wave approach to the shoreline. The highest tide level recorded at PY is less than 1 m above MHW (NOAA, 2017c). Therefore, the land boundary is considerably high in elevation to prevent the entire domain from getting wet (flooding) during simulations in order to avoid spurious predictions of littoral drift and shoreline evolution.

(c) In SC, the domain is 10.2 km longshore and 1.05 km cross-shore, extending from 30 m above MHW (300 m landward of the

shoreline) to 13 m below MHW. The mean wave height recorded over the 2009–2011 study period in SC is 1.02 m (standard deviation = 0.39). A 13 m depth boundary is, therefore, sufficiently deep to facilitate wave approach to the shoreline. The land boundary is also considerably high in elevation to ensure that the entire domain does not flood during simulations.

Each computational domain is split into two zones: nearshore and offshore. In NY and SC, the closure depth separates both zones. There are two indicators that are generally used to identify the closure depth in the absence of observed closure depth data in simple planform morphologies. In the first instance, the closure depth can be considered to be the depth along the beach profile beyond which we see no significant or abrupt change in bottom elevation (Kraus et al., 1998). This typically coincides with the most seaward depth contour that mirrors the shoreline shape, which provides a second qualitative indicator of the closure depth (Kaergaard and Fredsoe, 2013). This second qualitative indicator is applied in this paper to identify the closure depth in NY and SC, following Kaergaard and Fredsoe (2013). In complex planform morphologies, such as coral reef environments, the closure depth is more difficult to define and is generally considered to be the most seaward depth where reef substrate appears (Eversole and Fletcher, 2003). For this reason, the seaward boundary of the fringing reef network separates the nearshore and offshore zones in the domain defined for PR.

The computational mesh is generated in each domain using a maximum element area of 625 m² (25 m resolution) nearshore as a starting point, and 4 900 m² (70 m resolution) offshore. A finer resolution is adopted nearshore because it affects the representation of the nearshore bathymetry in the model, which influences the wave-current interactions that drive sediment transport. It is, therefore, important that the complexity and details of the nearshore bathymetry are well maintained in the computational mesh. Three factors have been considered in selecting the initial nearshore and offshore resolutions. These include process length scales of primary shoreline evolution drivers, numerical convergence, and computational feasibility (i.e. standard factors considered in mesh generation (Hardy et al., 1999)). The initial nearshore and offshore resolutions selected:

- (a) have a fine spatial resolution compared to the spatial scales over which primary drivers of shoreline evolution operate (Table 1). This is important to ensure that the model can resolve the key coastal processes that influence shoreline morphodynamics. Importantly, the nearshore and offshore resolutions selected also have a fine spatial resolution compared to the spatial scale of topo-bathymetric variations in each test site (Figs. 2–5). This ensures that the observed coastal profile morphology is well-maintained in the computational domain.
- (b) facilitate numerical convergence. Non-convergence is an indication that a model is unstable and do not fit the input data well. Ensuring numerical convergence is, therefore, a crucial step towards reducing numerical instabilities and ensuing uncertainties in model predictions.
- (c) create the finest mesh discretisation that is computationally feasible to apply MIKE21 in NY (i.e. the largest domain defined). Utilising four cores on a 2.8 GHz 16 core processor, a two-year simulation at this site using the initial mesh resolutions and computational domain defined took almost 24 h to complete (i.e. equivalent to 12 h per one-year simulation). From a coastal management decision-making perspective, whilst these simulation times are reasonable at the micro timescale, they would not be computationally practical or sustainable over the meso timescales that coastal managers are concerned with.

The same resolutions are used for mesh generation in each test site in order to objectively quantify the effects of mesh discretisation on shoreline evolution predictions in different coastal system

morphologies. The resulting meshes are finite volume discretisations with triangular elements, each containing a land, sea, and two connecting (open) boundaries (Fig. 8). There are 42 154, 20 878, and 13 032 triangular elements in the mesh generated for NY, PR, and SC, respectively.

Using the standard natural neighbour approach, the NY and PR mesh are each interpolated with their 2014 DEM, and the SC mesh with its 2009 DEM (Fig. 9). The natural neighbour interpolation approach preserves the original DEM data, which is necessary for ensuring that shoreline evolution predictions are based on observed coastal morphology.

3.5. Boundary conditions and model parameterisation

In each test site, the same principles are applied to parameterise MIKE21 for application. The tide and wave data obtained are forced at the sea boundary in the mesh and the connecting boundaries are kept open to facilitate littoral drift. The wind data obtained is forced over the model domain rather than at a particular boundary to account for the effects of wind on coastal hydrodynamics. All forcings are entered with a dampened interval of 2 h to prevent shock waves inside the model domain.

A zero-sediment flux gradient is specified at all mesh boundaries, except the land boundary. This is an open boundary condition that allows the same volume of sand in and out of the model domain as demanded by the changing hydrodynamics in the domain. A zero-sediment flux gradient prevents the sudden deposition or erosion of sediment at the open boundaries, ensuring the conservation of sediment mass and preventing instabilities from generating at the boundaries and propagating inside the model domain (Preston et al., 2018).

Each module in MIKE21 is parameterised to account for key coastal system features that are not represented by the boundary conditions specified above, as outlined in Table 4. The specifications of parameters in Table 4 follow the recommended guidelines for parameterising shoreline evolution models for application in sandy coastal systems (Manson, 2012; DHI, 2017).

MIKE21 ST calculates littoral drift rates by linear interpolation in a precomputed sediment transport table based on the hydrodynamic conditions appearing in the model domain. This table specifies the range of current speed, wave height, wave period, wave height to water depth ratio, the angle between current and waves, median grain size, sediment grading, and bed slope that may appear in the simulation. Errors accumulate in MIKE21 ST calculations if these conditions in a simulation are not within the range specified in the precomputed sediment transport table, causing unreliable shoreline evolution predictions. The precomputed sediment transport table defined for each test site, outlined in Table 5, takes into account the datasets obtained (Table 2) and is calibrated following Manson (2012).

The hard defences (e.g. groynes) in each test site are smaller than the size of elements in the meshes generated. A subgrid approach is, therefore, used to account for their effects in sediment transport simulations, as outlined in DHI (2017). In particular, all hard defences are discretised in the model domain as polyline features. The nodes forming these polylines have x,y coordinates, which specify the location and geometry of the hard defence structure, and an elevation (z) value relative to MHW.

3.6. Model sensitivity testing and calibration

3.6.1. Nearshore spatial discretisation

The mesh discretisation in the nearshore is an important specification in shoreline evolution models because it affects the representation of the nearshore bathymetry, which influences the wave-current interactions that drive sediment transport. Shoreline evolution predictions should be independent of the mesh discretisation in order for these predictions to be useful in guiding coastal management (Fringer et al.,

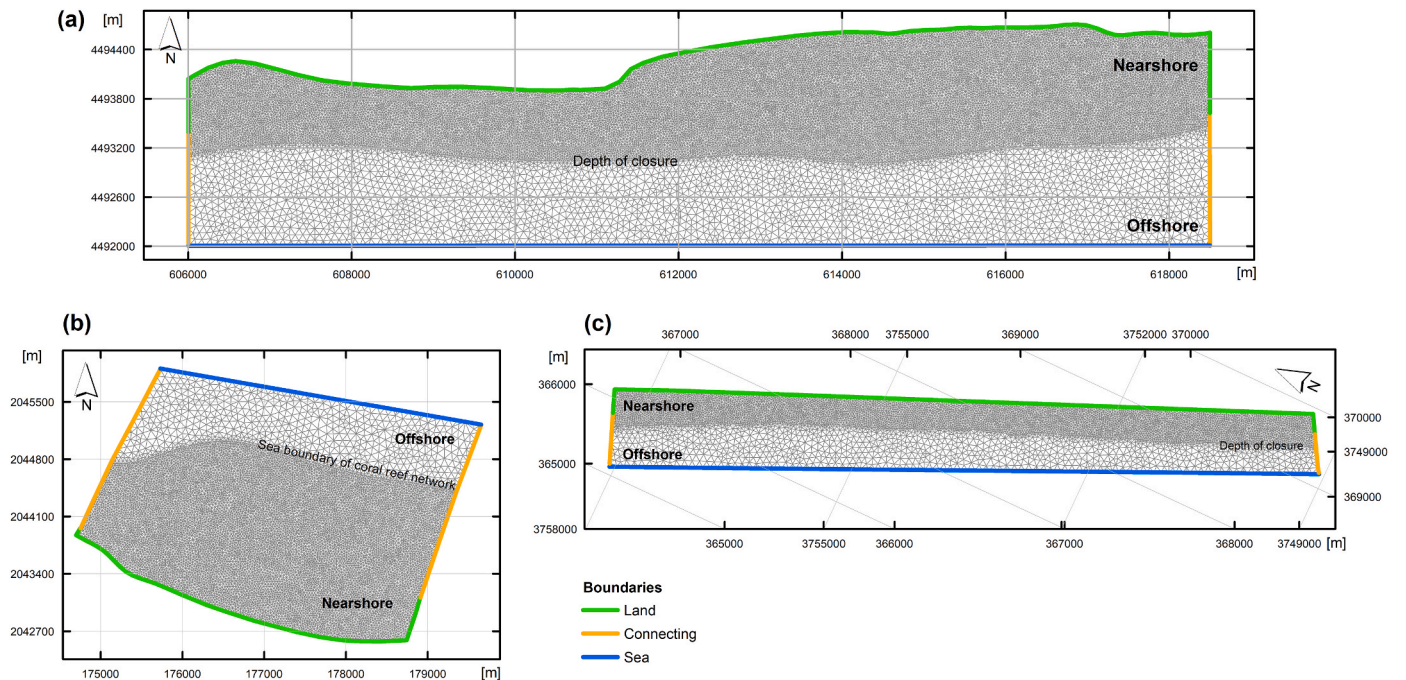


Fig. 8. Finite volume mesh generated for coastal sediment transport simulations in the New York (a), Puerto Rico (b) and Southern California (c) test site. Each mesh is projected in UTM coordinates (m).

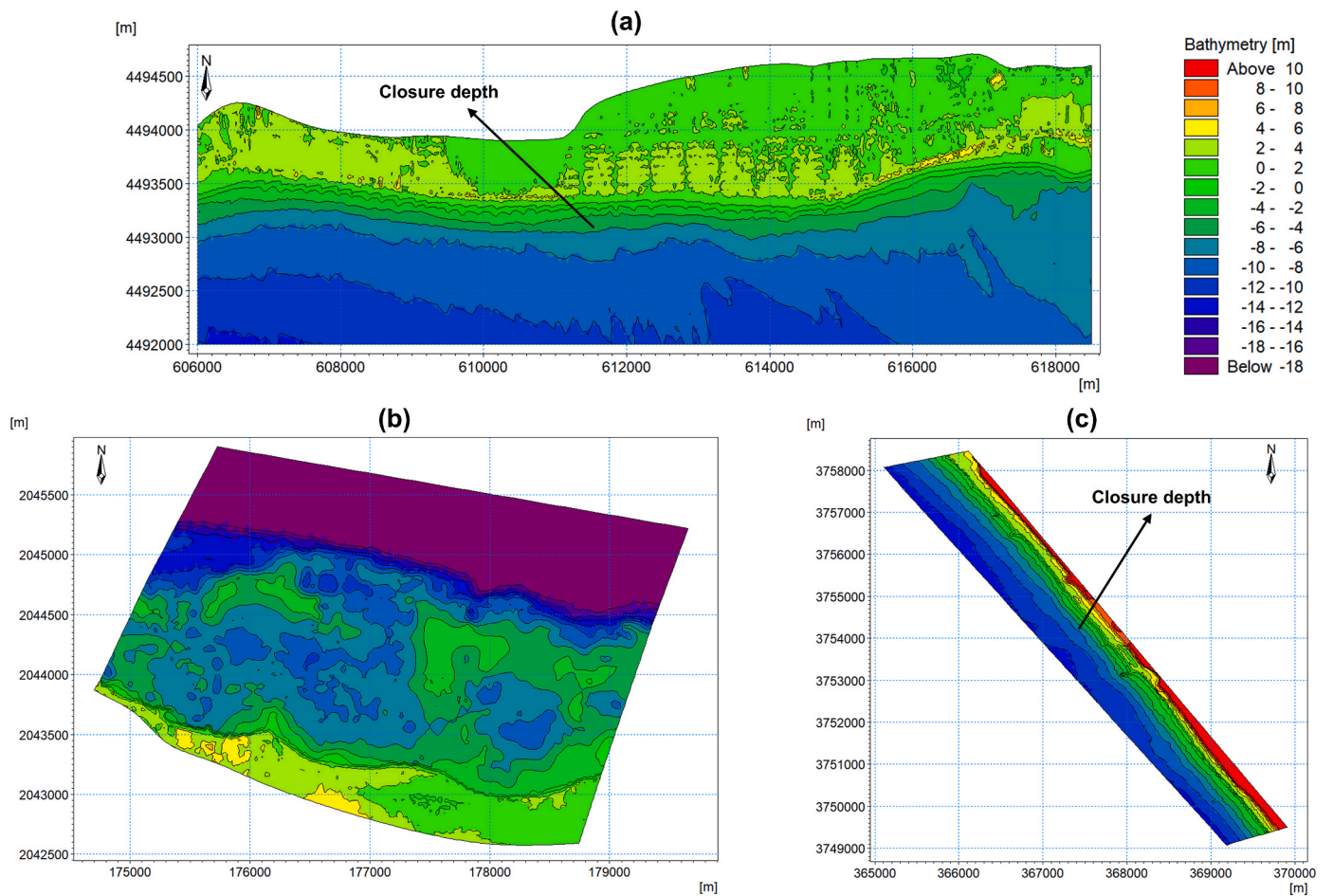


Fig. 9. 2D planimetric view of the New York (a), Puerto Rico (b), and Southern California (c) test site interpolated mesh. The general position of the closure depth contour in the New York and Southern California test site is indicated in (a) and (c), respectively. In the Puerto Rico test site, the closure depth varies longshore, as illustrated in Fig. 16.

Table 4

MIKE21 parameterisation for pre-calibration applications in each test site. NY = New York test site, PR = Puerto Rico test site, and SC = Southern California test site.

Input	Specifications
General	
Simulation period (model sensitivity testing <u>only</u>)	01-Jan-2014 to 01-Feb-2016 (NY) 01-Oct-2014 to 31-Mar-2016 (PR) 01-Jan-2009 to 02-Aug-2011 (SC)
Time step interval (output frequency)	86 400 s (daily)
MIKE21 HD	
Coriolis forcing	Varying in domain
Courant-Friedrich-Lévy (CFL) number	0.8
Density	Barotropic
Manning's n reciprocal	32 m ^{1/3} /s
Maximum time step	30 s
Minimum time step	0.01 s
Overtopping discharge ^a	0 m ³ /s/m
Smagorinsky coefficient (eddy viscosity)	0.28
Wave radiation stresses	Internally transfers from MIKE21 SW
Weir coefficient ^b	1.838 m ^{1/2} /s
Wind forcing	Wind speed and direction data
Wind friction (varies based on wind speed)	0.001255 to 0.002425
MIKE21 ST	
Critical Shields parameter	0.05
Grading coefficient	1.1
Grain diameter	0.2 mm
Flow/wave forcing	Internally transfers from MIKE21 SW
Maximum bed level change	10 m/day
Porosity	0.4
Relative sand density	2.65
Time step factor	1
MIKE21 SW	
Current conditions (speed and direction)	Internally transfers from MIKE21 HD
Maximum number of iterations	500
Nikuradse roughness	0.04 m
Reflection coefficient (structures)	0.5 (cross-shore structures in each test site) 1 (longshore structures in PR)
Spectral discretisation	360° rose
Water level conditions	Internally transfers from MIKE21 HD
MIKE21 SM	
Berm height	1.14 m (NY); 1.5 m (PR); 2 m (SC)
Closure depth	5.8 m (NY); 5.5 m (PR); 5 m (SC)
Maximum number of iterations	500
Sediment transport gradients	Internally transfers from MIKE21 ST

^a Used for longshore structures (e.g. seawalls and breakwaters) in the Puerto Rico test site.

^b Used for each test site's cross-shore structures (e.g. groynes).

2019). Herein, the independent mesh discretisation is defined as the mesh with the coarsest nearshore resolution that does not significantly affect model predictions even if the nearshore resolution gets finer. An independent mesh discretisation ensures that model predictions are due to the underlying physics solved and not the mesh resolution used. However, specifying an independent mesh discretisation is unbounded, nor are there any objective rules to guide mesh construction (Hardy et al., 1999; Williams and Esteves, 2017). Related studies tend to use the finest mesh discretisation that is computationally feasible or process length scales to define a mesh resolution without gauging the effects on model predictions. The importance of the nearshore spatial discretisation in shoreline evolution models is, therefore, not yet defined.

In each test site, the nearshore resolution in the mesh is successively coarsened from a maximum of 25 m–65 m at 5 m intervals in order to assess the sensitivity of shoreline evolution predictions to nearshore spatial discretisation. This procedure follows recommended guidelines for ensuring mesh independence (Hardy et al., 1999; Williams and Esteves, 2017). Eight additional meshes are, therefore, generated for each test site (Table 6). The range of nearshore discretisations (25 m–65 m) considered have a fine spatial resolution compared to the spatial scales over which the primary drivers of shoreline evolution operate

Table 5

Calibrated sediment transport table for shoreline evolution simulations in each test site. The first value, spacing, and the number of points in each axis define the range of each condition that may appear during a simulation and influence sediment transport rates. The first value is the minimum value. The second value in each axis, except grain size, is the “First value + Spacing” and so forth. The second value for grain size is the “First value × Spacing” and so on.

Sediment table axis	First value	Spacing	No. of points
New York test site			
Current speed (m/s)	0.01	0.8	5
Wave height (m)	0.19	2	4
Wave period (s)	2.35	2	8
Wave height to water depth ratio	0.01	10	10
Angle between current and waves (deg)	0	30	12
Median grain size (mm)	0.2	2	8
Sediment grading	1.1	0.15	5
Bed slope – current direction (rad)	−0.01	0.7	2
Bed slope – perpendicular to current direction (rad)	−0.02	0.7	2
Puerto Rico test site			
Current speed (m/s)	0.01	0.8	5
Wave height (m)	0.1	1	4
Wave period (s)	3	4	8
Wave height to water depth ratio	0.01	10	10
Angle between current and waves (deg)	0	30	12
Median grain size (mm)	0.2	2	8
Sediment grading	1.1	0.15	5
Bed slope – current direction (rad)	−0.01	0.7	2
Bed slope – perpendicular to current direction (rad)	−0.02	0.7	2
Southern California test site			
Current speed (m/s)	0.01	1	4
Wave height (m)	0.1	1	5
Wave period (s)	3	3	8
Wave height to water depth ratio	0.1	11	10
Angle between current and waves (deg)	0	30	12
Median grain size (mm)	0.2	2	8
Sediment grading	1.1	0.15	3
Bed slope – current direction (rad)	−0.01	0.7	2
Bed slope – perpendicular to current direction (rad)	−0.02	0.7	2

(Table 1). As previously mentioned, this is important to ensure that the model can resolve the key coastal processes that influence shoreline morphodynamics. In each additional mesh, the maximum offshore resolution is kept constant at 70 m. Figs. 10–12 present the finest, median, and coarsest mesh generated for NY, PR, and SC, respectively. All additional meshes are interpolated following the procedures in Section 3.4.

In each test site, nine successive simulations are carried out, starting with the finest mesh and ending with the coarsest mesh generated. Model default values of the various parameters are used in these pre-calibration simulations (DHI, 2017). This is important for identifying the independent mesh discretisation for subsequent shoreline evolution simulations. The effects of coarsening nearshore spatial discretisation on shoreline evolution predictions are quantified using the Brier Skill Score (details in Section 3.7), and the results are used to identify the independent mesh discretisation.

3.6.2. DEM resolution

The DEM used for mesh interpolation defines the bed surface elevation that influences wave-current interactions and sediment transport simulations. An overly coarse DEM may exclude intricate sea-floor features and affect littoral drift calculations and associated shoreline evolution predictions. However, there are no defined guidelines on the optimal DEM resolutions for simulating shoreline evolution.

Using the nearest neighbour resampling method in ArcGIS, the NY and PR 2014 DEM is resampled from 3 m to 9, 27, 81, 90, 100, and 500 m, and the SC 2009 DEM from 10 m to 27, 81, 90, 100, and 500 m (Tables 7–9). These resolutions correspond to the range of DEM

Table 6

Details of all meshes generated for sensitivity testing in each test site. Mesh25 refers to a mesh with a nearshore spatial discretisation of 25 m and so on.

Characteristic	Mesh								
	25	30	35	40	45	50	55	60	65
Nearshore max. element area (m ²)	625	900	1 225	1 600	2 025	2 500	3 025	3 600	4 225
Offshore max. element area (m ²)	4 900 →								
Nearshore max. resolution (m)	25	30	35	40	45	50	55	60	65
Offshore max. resolution (m)	70 →								
Total nodes									
New York test site	21 456	15 874	12 035	9 684	8 222	7 203	6 396	5 776	5 235
Puerto Rico test site	10 623	7 661	5 706	4 425	3 648	3 089	2 717	2 430	2 191
Southern California test site	6 791	5 061	3 771	3 052	2 670	2 353	2 109	1 957	1 825
Total elements									
New York test site	42 154	31 085	23 547	18 884	15 963	13 934	12 323	11 116	10 010
Puerto Rico test site	20 878	14 974	11 146	8 625	7 071	5 953	5 209	4 635	4 157
Southern California test site	13 032	9 646	7 172	5 755	4 994	4 366	3 889	3 594	3 334

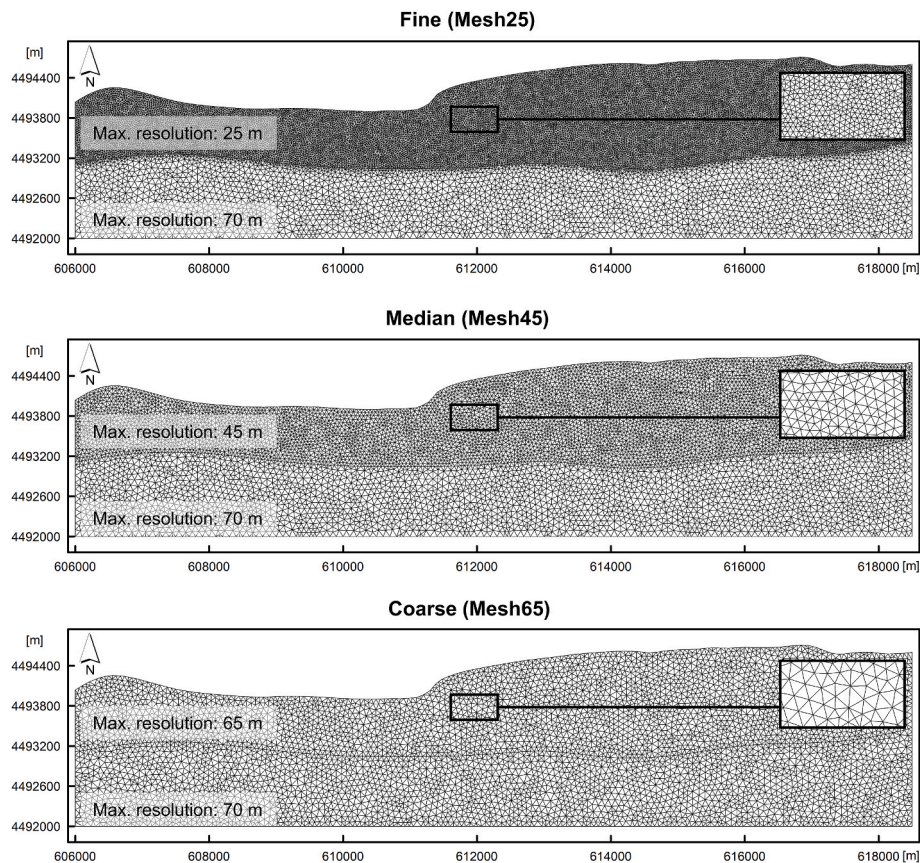


Fig. 10. The fine, median, and coarse mesh used for the mesh independence study in the New York test site. Each mesh is projected in UTM coordinates (m).

resolutions (open-source and commercial) that are available globally. The nearest neighbour resampling method is selected because it preserves the original DEM data, which is important for maintaining observed coastal features.

In each test site, model sensitivity to DEM resolution is assessed by running successive simulations using (a) their independent mesh discretisation interpolated with coarsening (resampled) DEMs and (b) default model values for all other inputs. The effects of coarsening DEM resolution on shoreline evolution predictions are subsequently quantified using the Brier Skill Score (see Section 3.7).

3.6.3. Free parameters

Free parameters are constants in a simulation whose values are difficult to define *a priori* (e.g. friction). These parameters can significantly affect model predictions, and their specification in shoreline

evolution models typically require calibration bounded by physically realistic values. Following Manson (2012), a stepwise approach is used to calibrate and assess the sensitivity of shoreline evolution predictions in each test site against five parameters:

- bed resistance based on Manning's n reciprocal (m^{1/3}/s), which affects the flow rate and wave dissipation, influencing sediment transport and redistribution over the mesh bathymetry.
- sand porosity, which affects the shoreface morphology by influencing the concentration of suspended sediments.
- sand grain diameter, which influences the sediment transport rate and volume of sediment that can become entrained in the flow. As sand grain size increases, littoral drift decreases.

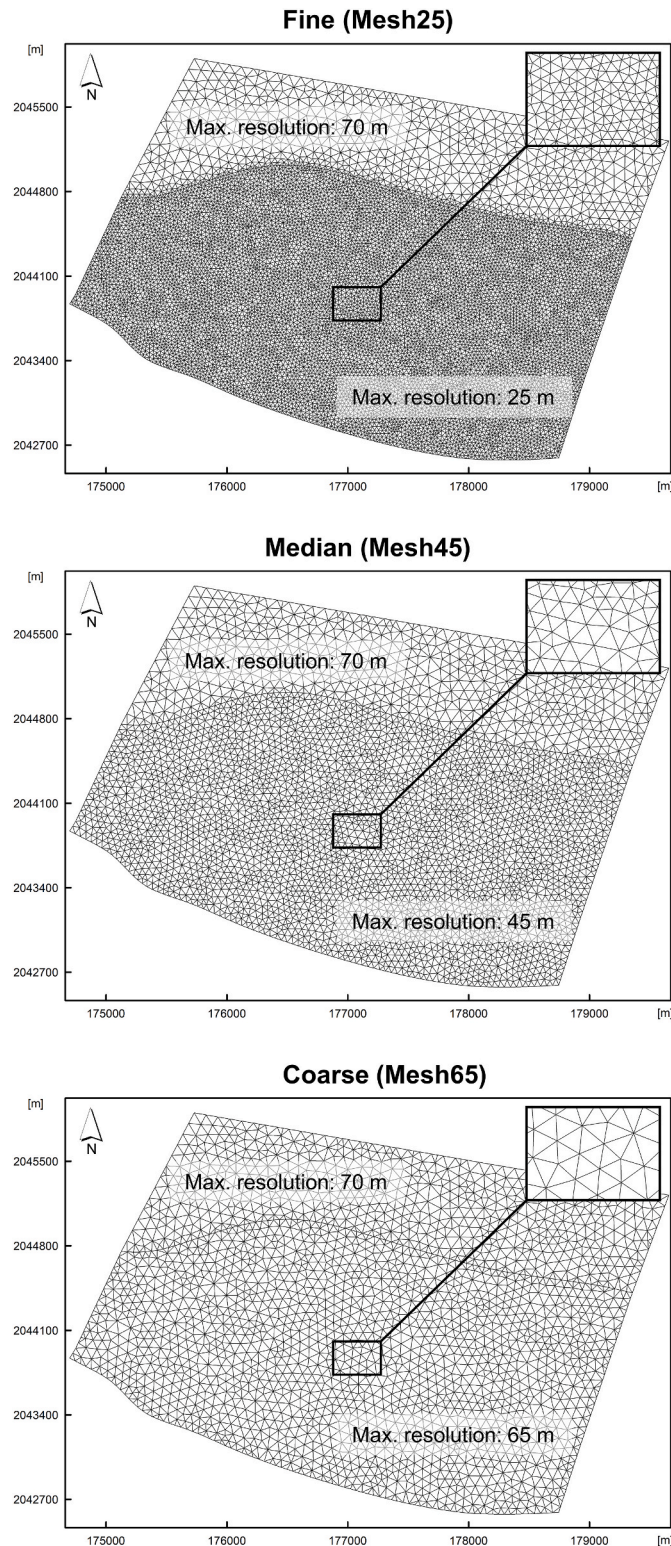


Fig. 11. The fine, median, and coarse mesh used for the mesh independence study in the Puerto Rico test site. Each mesh is projected in UTM coordinates (m).

- (d) sediment grading coefficient. Well-sorted sediments have smaller grains and are less resistant to flow than poorly sorted sediments with mixed grain sizes.

- (e) the weir coefficient ($m^{1/2}/s$) of hard defences, which controls the overtopping discharge at hard defences, affecting sediment redistribution and flow around structures.

The stepwise approach tunes (and calibrate) one parameter at a time. Bed resistance is first calibrated to identify an appropriate Manning's n reciprocal for later simulations, followed by sand porosity, sand grain diameter, sediment grading coefficient, and weir coefficient. Calibrating one parameter at a time is useful for identifying the key parameters that cause the largest errors in shoreline evolution predictions. This knowledge is fundamental for understanding (and refining) the intrinsic behaviour of shoreline evolution models (Manson, 2012; Williams and Esteves, 2017). Importantly, the calibration process carried out is based on established ranges for each of the above parameters (Table 10). This, therefore, reduces the subjectivity in the model calibration process, ensuring that the shoreline evolution predictions obtained are bounded by *physically realistic* estimates of each parameter calibrated (Manson, 2012). All calibration simulations are based on the independent mesh discretisation. This reduces the uncertainty in ensuing shoreline evolution predictions, ensuring that the predictions obtained are based on the underlying physics resolved in the model and are not due to the mesh specifications. The effects of the stepwise calibration on shoreline evolution predictions in each test site are quantified using the Brier Skill Score (see Section 3.7). The results are used to define the relative influence of each free parameter above on shoreline evolution predictions in sandy coastal systems.

3.7. Model verification

2 449 cross-shore transects in NY, 702 in PR, and 1 941 in SC are used to map the observed and predicted shoreline positions (x, y) over the associated two-year study period. All transects generated are spaced every 5 m longshore. The observed and predicted shoreline positions in each transect are used to quantify the accuracy of shoreline evolution predictions using the Brier Skill Score (BSS):

$$BSS = 1 - \frac{\sum (Sh_{obs} - Sh_{pred})^2}{\sum (Sh_{obs} - Sh_{init})^2} \quad \text{Eqn. 1}$$

where Sh_{init} is the initial shoreline position observed at the start of the study period per transect, Sh_{pred} is the predicted shoreline position at the end of the study period per transect, and Sh_{obs} is the observed shoreline position at the end of the study period per transect. BSS ranges from $-\infty$ to 1. A BSS of 1 indicates perfect agreement between Sh_{obs} and Sh_{pred} , 0 indicates that Sh_{pred} is closer to Sh_{init} , and a negative BSS indicates that Sh_{pred} is further away from Sh_{obs} . Sutherland et al. (2004) BSS classification scheme, which classifies a score of 1 to 0.5 as excellent, 0.5 to 0.2 as good, 0.2 to 0.1 as reasonable, 0.1 to 0 as poor, and ≤ 0 as bad, is adopted in this paper.

Additionally, descriptive statistics and spatial line plots are used to quantify and visualise the differences between shoreline evolution observations and predictions longshore. These additional measures enable a more robust interpretation of all BSS estimations.

4. Results and analysis

Results show that shoreline evolution predictions in each test site are affected by nearshore spatial discretisation, DEM resolution, bed friction, and sediment properties (size, porosity, and grading) (Fig. 13; Table 11). The weir coefficient of hard structures has a negligible effect on these predictions. A closer inspection of these results indicates that (a) the optimal specifications of these inputs correspond to observed coastal geomorphology (Section 4.1), and (b) the hybrid 2D/one-line modelling approach is restricted to simple planform morphologies (Section 4.2).

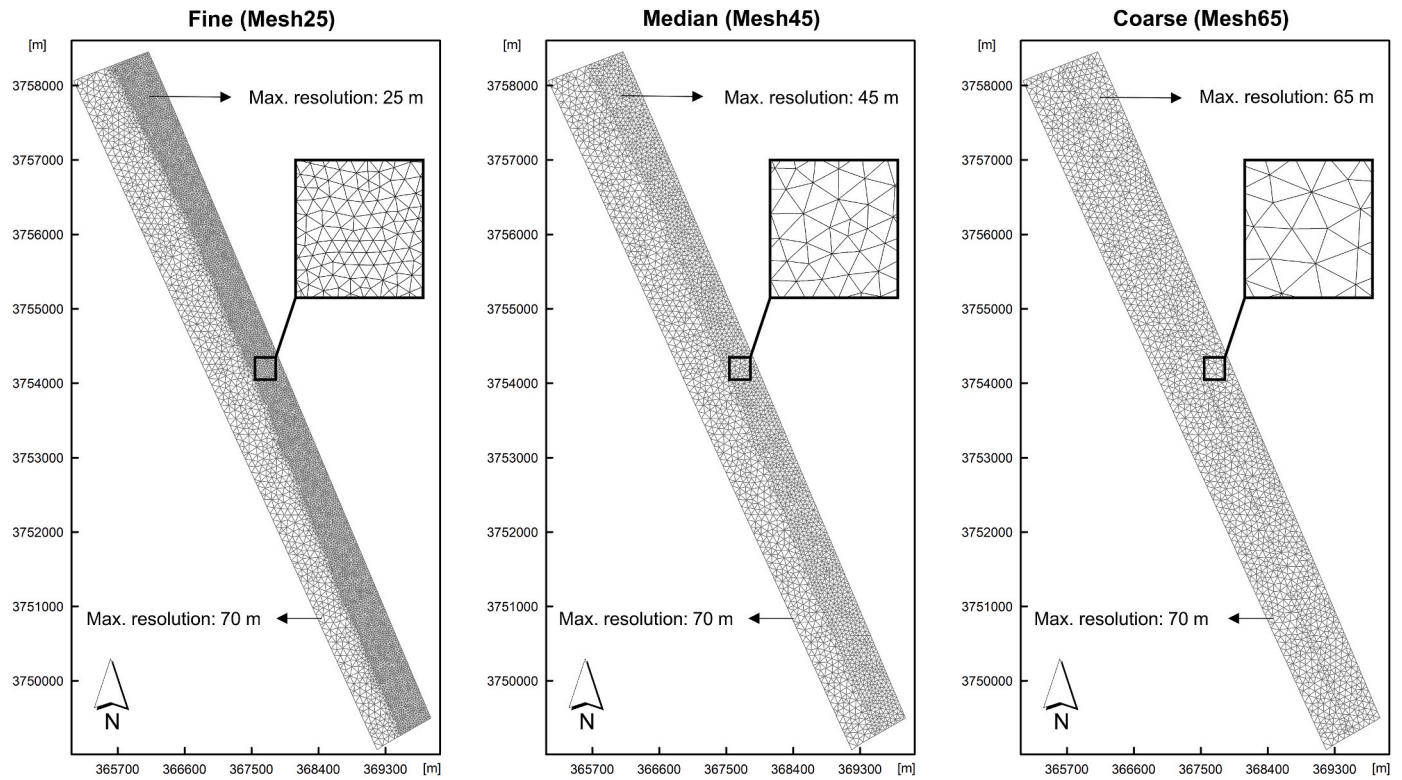


Fig. 12. The fine, median, and coarse mesh used for the mesh independence study in the Southern California test site. Each mesh is projected in UTM co-ordinates (m).

Table 7

Elevation and slope characteristics in the DEMs (original and resampled) used for sensitivity testing in the New York test site.

Characteristic		Original DEM	Resampled DEMs					
Resolution (m)		3	9	27	81	90	100	500
Elevation	Minimum (m)	−12.46	−12.46	−12.45	−12.37	−12.19	−12.19	−12.11
	Maximum (m)	8.42	8.42	7.89	7.42	5.68	6.25	4.14
	Mean (m)	−4.3	−4.28	−4.33	−4.32	−4.11	−4.15	−5.26
	Standard deviation	5.2	5.2	5.2	5.2	5.17	5.19	5.13
Slope	Minimum (deg.)	0	0	0	0.01	0.01	0	0.01
	Maximum (deg.)	31.48	15.62	5.21	3.71	5.51	3.89	0.77
	Mean (deg.)	1.1	0.83	0.56	0.44	0.46	0.45	0.32
	Standard deviation	1.58	1	0.61	0.52	0.57	0.54	0.21

Table 8

Elevation and slope characteristics in the DEMs (original and resampled) used for sensitivity testing in the Puerto Rico test site.

Characteristic		Original DEM	Resampled DEMs					
Resolution (m)		3	9	27	81	90	100	500
Elevation	Minimum (m)	−50.52	−50.52	−50.49	−50.67	−49.14	−50.2	−46.7
	Maximum (m)	7.87	7.67	7.04	6.93	6.12	5.73	4.83
	Mean (m)	−11.98	−12.08	−12.24	−12.66	−12.22	−12.38	−11.13
	Standard deviation	12.73	12.81	12.92	13.21	12.87	13.01	12.06
Slope	Minimum (deg.)	0	0	0.01	0.03	0.03	0.02	0.03
	Maximum (deg.)	50.59	25.72	11.06	5.62	5.16	4.72	2.43
	Mean (deg.)	2.03	1.89	1.66	1.35	1.3	1.29	0.96
	Standard deviation	2.16	1.76	1.42	1.11	1.08	1.04	0.77

4.1. Sensitivity and calibration

We can see a clear optimal range of nearshore discretisation for modelling shoreline evolution in each test site. The coarsest optimal nearshore discretisation is finer in SC (30 m) than in NY and PR (45 m) (Fig. 13a). This finding is linked to SC having a steeper average coastal profile (slope = 2.68%) than NY (slope = 1.82%) and PR (slope =

1.75%) (Table 12; Fig. 5). The nearshore discretisation influences how well the observed coastal profile morphology is represented in the model domain. For instance, the coastal profile smoothens in response to coarsening nearshore discretisation. As a result, steep coastal profiles become numerically gradient over a smaller range of nearshore discretisations than gentle profiles because of their larger bed topography range, which plausibly explains these results.

Table 9

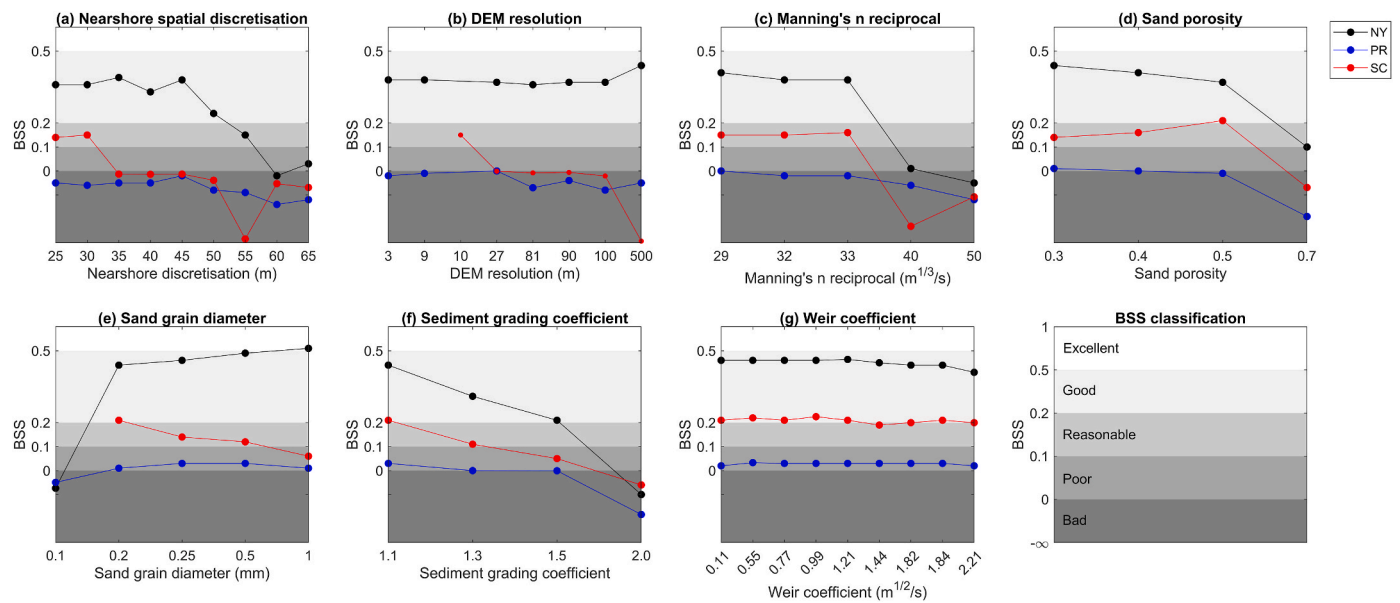
Elevation and slope characteristics in the DEMs (original and resampled) used for sensitivity testing in the Southern California test site.

Characteristic		Original DEM	Resampled DEMs				
Resolution (m)		10	27	81	90	100	500
Elevation	Minimum (m)	-14.06	-14.19	-13.78	-14.09	-13.64	-13
	Maximum (m)	31.88	28.53	28.81	26.26	31.57	21.79
	Mean (m)	-3.98	-4.63	-4.16	-5.03	-3.23	-4.08
	Standard deviation	8.57	7.92	8.41	7.52	9.37	8.37
Slope	Minimum (deg.)	0	0	0.04	0.02	0.08	0.55
	Maximum (deg.)	32.8	20.21	10.54	9.36	11.32	3.18
	Mean (deg.)	2.06	1.88	1.93	1.76	2.1	1.77
	Standard deviation	2.8	2.25	1.99	1.76	2.1	0.81

Table 10

Calibration inputs. Bold values are model default values.

Input	Units	Established range	Reference	Calibration variations
Nearshore discretisation	m	N/A	N/A	25, 30, 35, 40, 45, 50, 55, 60, 65
Manning's n (Sandy beaches)	$m^{1/3}/s$	reciprocals: 28–50	Chow (1959)	28, 29, 32 , 33, 40, 50
Sand grain diameter	mm	0.0625–0.125 (very fine)	Wentworth (1922)	0.1, 0.2 , 0.25, 0.5, 1
		0.0125–0.25 (fine)		
		0.25–0.5 (medium)		
		0.5–1 (coarse)		
		1–2 (very coarse)		
Sand porosity	N/A	0.3–0.7	Nimmo (2013)	0.3, 0.4 , 0.5, 0.7
Sediment grading coefficient	N/A	<1.27 (very well sorted)	Folk and Ward (1957)	1.1 , 1.3, 1.5, and 2
		1.27–1.4 (well sorted)		
		1.41–1.99 (moderately sorted)		
		2–3.99 (poorly sorted)		
		4–15.99 (very poorly sorted)		
Weir coefficient	$m^{1/2}/s$	≥16 (extremely poorly sorted)	Horton (1906)	0.11, 0.55, 0.77, 0.99, 1.21, 1.44, 1.82, 1.838 , 2.21
		0.11–0.27 (Lateral structure)		
		0.3–1.71 (Broad crested structure)		
		1.77–2.26 (Ogee crested structure)		
		1.71–1.82 (Sharp crested structure)		

**Fig. 13.** Accuracy of shoreline evolution predictions in response to variations in boundary conditions in the New York (NY), Puerto Rico (PR), and Southern California (SC) test site. BSS is Brier Skill Score. The BSS classification should be interpreted as outlined in the text (Section 3.7).

We can also see a clear optimal range of DEM resolution for mesh interpolation and associated shoreline evolution simulations in NY and PR (Fig. 13b). In SC, the results are inconclusive as there is no indication of an optimal DEM resolution range since there is a considerable drop in BSS after the finest DEM. The coarsest optimal DEM resolution is ≤ 100 m in NY, ≤ 27 m in PR, and possibly <10 m in SC (Fig. 13b; Table 11).

These results are also linked to observed coastal profile morphology. NY and PR have a coarser optimal range of DEM resolutions than SC plausibly because their average coastal profile is more gentle sloping (Table 12; Fig. 5). However, PR has a finer optimal DEM resolution range than NY because it has a non-uniform bathymetry in response to coral reefs (Fig. 5 a – b). As a result, PR has more longshore and cross-

Table 11

Statistical summary of shoreline change observed and predicted in response to variations in boundary conditions in the New York (NY), Puerto Rico (PR), and Southern California (SC) test site.

Input	Specification	Mean net change (m)			Mean absolute change (m)			Brier Skill Score		
		NY	PR	SC	NY	PR	SC	NY	PR	SC
Observed shoreline change (m)	–	–0.01	3.22	15.15	1.16	5.03	15.98	–	–	–
Nearshore discretisation (m)	25	–0.15	0.13	0.19	0.87	1.18	8.14	0.36	–0.05	0.14
	30	–0.19	0.14	0.67	0.87	1.23	8.5	0.36	–0.06	0.15
	35	–0.18	0.13	0.42	0.88	1.25	9.05	0.39	–0.05	–0.16
	40	–0.17	0.17	0.40	0.89	1.23	10.17	0.33	–0.05	–0.17
	45	–0.17	0.13	1.09	0.88	1.25	10.45	0.38	–0.02	–0.16
	50	–0.19	0.13	1.35	0.96	1.41	11.26	0.24	–0.08	–0.47
	55	–0.18	0.15	1.7	1.01	1.29	12.82	0.15	–0.09	–3.41
	60	–0.2	0.13	0.93	1.17	1.41	11.12	–0.02	–0.14	–0.64
DEM resolution (m)	65	–0.21	0.14	–0.07	1.11	1.41	10.77	0.03	–0.12	–0.83
	3	–0.17	0.13	–	0.88	1.25	–	0.38	–0.02	–
	9	–0.17	0.17	–	0.87	1.21	–	0.38	–0.01	–
	10	–	–	0.67	–	–	8.5	–	–	0.15
	27	–0.16	0.15	0.08	0.86	1.13	7.76	0.37	0.00	–0.02
	81	–0.18	0.14	–0.24	0.87	1.21	8.11	0.36	–0.07	–0.18
	90	–0.17	0.14	–0.22	0.86	1.30	7.98	0.37	–0.04	–0.14
	100	–0.19	0.14	–1.18	0.86	1.18	8.43	0.37	–0.08	–0.48
Manning's n reciprocal ($\text{m}^{1/3}/\text{s}$)	500	–0.2	0.11	–1.93	0.82	0.96	29.76	0.44	–0.05	–6.75
	29	–0.17	0.12	0.67	0.83	1.13	8.38	0.41	0	0.15
	32	–0.17	0.13	0.67	0.88	1.25	8.5	0.38	–0.02	0.15
	33	–0.17	0.16	0.89	0.89	1.28	8.57	0.38	–0.02	0.16
	40	–0.17	0.18	4.39	1.16	1.54	15.16	0.01	–0.06	–2.31
	50	–0.21	0.19	2.91	1.26	1.86	13.08	–0.05	–0.12	–1.08
	0.3	–0.17	0.14	0.63	0.79	0.99	8.25	0.44	0.01	0.14
	0.4	–0.17	0.13	0.89	0.83	1.25	8.57	0.41	0	0.16
Sand porosity	0.5	–0.17	0.14	1.29	0.89	1.3	9.06	0.37	–0.01	0.21
	0.7	–0.16	0.19	3.46	1.19	2.19	14.52	0.1	–0.19	–2.07
	0.1	0.46	1.13	–	11.85	11.76	–	–73.66	–9.85	–
Sand grain diameter (mm)	0.2	–0.17	0.14	1.29	0.79	0.99	9.06	0.44	0.01	0.21
	0.25	–0.16	0.11	0.59	0.75	0.82	8.52	0.46	0.03	0.14
	0.5	–0.17	0.1	0.56	0.66	0.51	6.77	0.49	0.03	0.12
	1	–0.19	0.06	0.6	0.62	0.28	6.79	0.51	0.01	0.06
	1.1	–0.17	0.11	1.29	0.79	0.82	9.06	0.44	0.03	0.21
Sediment grading coefficient	1.3	–0.15	0.13	0.47	0.97	1.255	8.55	0.31	–0.02	0.11
	1.5	–0.15	0.23	0.4	1.41	2.14	8.74	–0.21	–0.17	0.05
	2	1.71	1.84	0.25	43.33	27.14	9.7	–1 169.67	–55.01	–0.06
	0.11	–0.16	0.11	1.39	0.76	0.82	9.06	0.46	0.02	0.21
Weir coefficient ($\text{m}^{1/2}/\text{s}$)	0.55	–0.16	0.11	1.38	0.76	0.82	8.96	0.46	0.03	0.22
	0.77	–0.16	0.11	1.35	0.76	0.82	9.08	0.46	0.03	0.21
	0.99	–0.16	0.11	1.37	0.76	0.82	8.81	0.46	0.03	0.22
	1.21	–0.16	0.11	1.25	0.76	0.82	9.02	0.46	0.03	0.21
	1.44	–0.17	0.11	1.37	0.77	0.82	9.27	0.45	0.03	0.19
	1.82	–0.17	0.11	1.38	0.79	0.82	9.23	0.44	0.03	0.2
	1.838	–0.17	0.11	1.29	0.79	0.82	9.06	0.44	0.03	0.21
	2.21	–0.16	0.12	1.26	0.82	0.83	9.2	0.41	0.02	0.2

Table 12

Characteristics of the active coastal profile slope in each test site. Descriptive statistics below are based on the active coastal profile slope in transects every 5 m longshore.

Slope (%)	New York test site	Puerto Rico test site	Southern California test site
Minimum	1.19	1.13	2.08
Maximum	2.42	2.28	4
Mean	1.82	1.75	2.68
Standard deviation	0.22	0.26	0.42

shore fluctuations in bed topography than NY over equivalent spatial distances (Fig. 5 a – b). Therefore, PR coastal profile morphology becomes numerically gradient over a smaller DEM resolution range than NY coastal profile morphology (Fig. 14).

An interesting observation is that DEM resolutions up to 100 m seem appropriate for simulating shoreline evolution in simple planform morphologies with a relatively flat bed surface as in NY (Fig. 13b). This finding implicitly implies that coarse open-source DEMs, such as the Shuttle Radar Topography Mission (SRTM) (90 m resolution), may be

sufficient for simulating shoreline evolution in relatively flat and gentle sloping morphologies. In this paper, the sensitivity of shoreline evolution predictions to DEM resolution is assessed by resampling high-quality DEMs using the nearest neighbour approach, which typically preserves the high-quality measurements from the original DEM. The resampled (coarser) DEMs used for sensitivity testing in each test site may, therefore, contain higher precision measurements than open-source DEMs of the same spatial resolution (Seenath, 2018). The sensitivity results presented here, thus, cannot be used to make concrete inferences on the potential effects of DEM quality on shoreline evolution predictions.

As with the nearshore discretisation, there is a clear optimal range of Manning's n reciprocal for simulating shoreline evolution in each test site. The most accurate Manning's n reciprocal is 29 $\text{m}^{1/3}/\text{s}$ in NY and PR, and 33 $\text{m}^{1/3}/\text{s}$ in SC (Fig. 13c; Table 11). These reciprocals correspond to a Manning's n of ~ 0.03 , which is more representative of sandy coastal systems, characteristic of each test site, than Manning's n reciprocals of 40 and 50 $\text{m}^{1/3}/\text{s}$ (Seenath, 2018). Manning's n reciprocals of 40 and 50 $\text{m}^{1/3}/\text{s}$ are more representative of open water bodies (Mattocks and Forbes, 2008), which plausibly explains the associated decline in shoreline evolution prediction accuracy (Fig. 13c; Table 11).

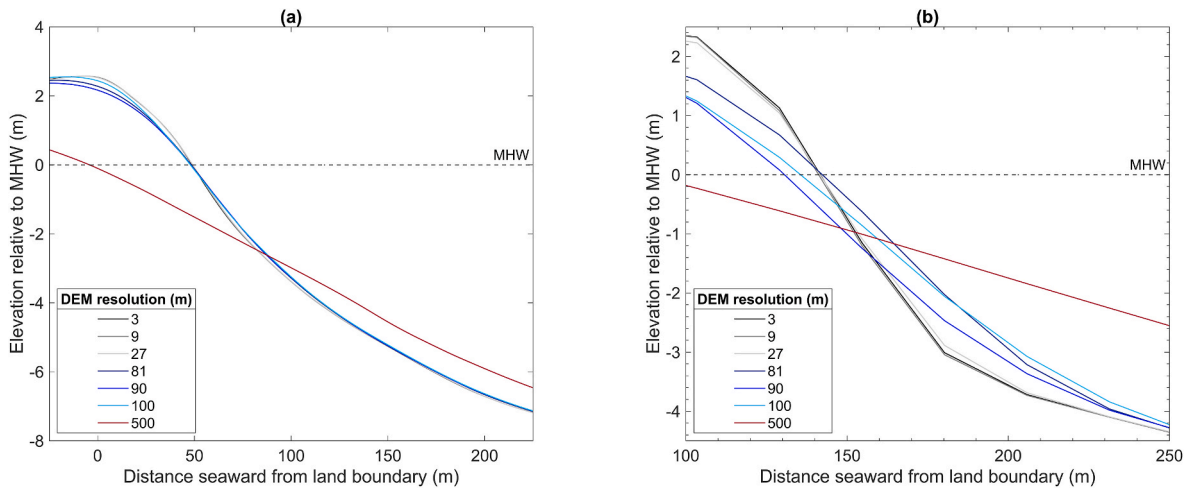


Fig. 14. Effects of coarsening DEM resolution on the coastal profile morphology in the New York (a) and Puerto Rico (b) test site.

We can see an almost clear linear relationship between increasing sand grain diameter and shoreline evolution prediction accuracy in NY and SC. In particular, there is a noticeable improvement in shoreline evolution prediction accuracy with increasing sand grain diameter in NY. The inverse is true at SC. In PR, we start to see an almost parabolic relationship developing between increasing sand grain diameter and shoreline evolution prediction accuracy. As a result, the most accurate sand grain diameter for modelling shoreline evolution is 0.2 mm in SC, 0.25 and 0.5 mm in PR, and 1 mm in NY (Fig. 13e; Table 11). A sand grain diameter of 0.2 mm is characteristic of the fine-grained beach sediments in SC, and 0.25 and 0.5 mm are both characteristic of the medium-grained beach sediments in PR (Kaye, 1959; Farnsworth and Warrick, 2007). However, a sand grain diameter of 1 mm is not characteristic of the NY site where the median grain size is ~ 0.2 mm (USACE and NYSDEC, 2015). Therefore, 0.2 mm is considered to be the optimal sand grain diameter in NY to avoid having a right model for the wrong reasons, where right refers to the best match between observed and predicted shoreline evolution and wrong refers to physically unrealistic parameter values of the conceptual model describing the NY morphology. Coastal management can be adversely affected, with implications (ineffectiveness or worsening of coastal change), if shoreline evolution predictions are not based on observed coastal morphology. Caution is thus necessary when identifying calibrated values of key model inputs.

There also seems to be a linear relationship between declining shoreline evolution prediction accuracy and increasing sediment porosity and grading coefficient in each test site. The optimal sand porosity for modelling shoreline evolution ranges from 0.3 in NY and PR to 0.5 in SC (Fig. 13d; Table 11). These values fall within the range of fine (0.26–0.53) and medium (0.29–0.49) grained sand porosities, therefore are characteristic of sand grain diameters in each test site. The optimal sediment grading coefficient is 1.1 in each test site (Fig. 13f), which is representative of their very well sorted beach sediments (Terry et al., 1956; Kaye, 1959; USACE and NYSDEC, 2015).

Analysing and comparing the model sensitivity results from each test site reveal that the optimal specifications of model inputs for simulating shoreline evolution generally correspond to observed coastal system morphology and processes. These sensitivity results highlight the importance of carefully considering coastal system features when parameterising shoreline evolution models.

4.2. Applicability of the hybrid 2D/one-line approach

A key observation from the modelling results is that the hybrid 2D/one-line approach, applied through MIKE21, appears to work best in

simple planform morphologies, where the active coastal profile is stable. This inference stems from the calibrated shoreline evolution predictions having a BSS of 0.5 (good) in NY, 0.0 in PR (bad), and 0.2 (borderline good) in SC. Fig. 15 corroborates these BSS values by illustrating that:

- There is a generally good fit between the longshore variations (trends and direction) in shoreline evolution observed and predicted in NY following calibration (Fig. 15a), further evident by a statistically significant Spearman correlation ($r = 0.42$, $p = 0.00$). Importantly, the signs in the mean net shoreline change (MNC) observed and predicted in NY are consistent (negative), indicating that shoreline evolution observations and predictions move in the same direction. Movements in the same direction are a good indication that the model is able to replicate observed trends. However, the hybrid 2D/one-line approach underpredicts shoreline change, evident from the observed mean absolute change (1.16 m) being larger than the predicted (0.76 m). This can be attributed to several factors, including mesh quality, data quality, or even the computational structure of the model (Section 5). It is not the aim of this paper to verify the cause of model prediction accuracy/error, but rather to test the response of the hybrid 2D/one-line approach to variations in inputs and morphology.
- The hybrid 2D/one-line approach fails to predict observed shoreline change in PR despite significant calibration attempts (Fig. 15b), further evident by a statistically insignificant Spearman correlation ($r = 0.02$, $p = 0.53$). Shoreline evolution predictions in PR vary closely around zero metres (-4 to 5.7 m) longshore compared to associated observations (-11.26 to 16.23 m). The predicted MNC in PR is thus negligible (0.11 m) relative to the observed (3.22 m), hence the bad BSS of 0.0. These considerable differences plausibly stem from the inability of the hybrid 2D/one-line approach to handle the longshore variability of the closure depth in PR (Fig. 16; Section 5.4). This approach assumes shore-parallel contours in the shoreline morphology update, which means that the closure depth is considered constant longshore. In line with these assumptions, a 5.5 m closure depth was specified in PR, which inevitably averages out the longshore variability of the closure depth (and the active coastal profile) at the site. The 5.5 m depth contour is the deepest shore-parallel contour landward of the reefs. In coral reef environments, the first occurrence of reef substrate indicates the closure depth, which means that the closure depth varies naturally longshore in these environments since the spatial distribution of reef substrate tends to be irregular (Eversole and Fletcher, 2003).

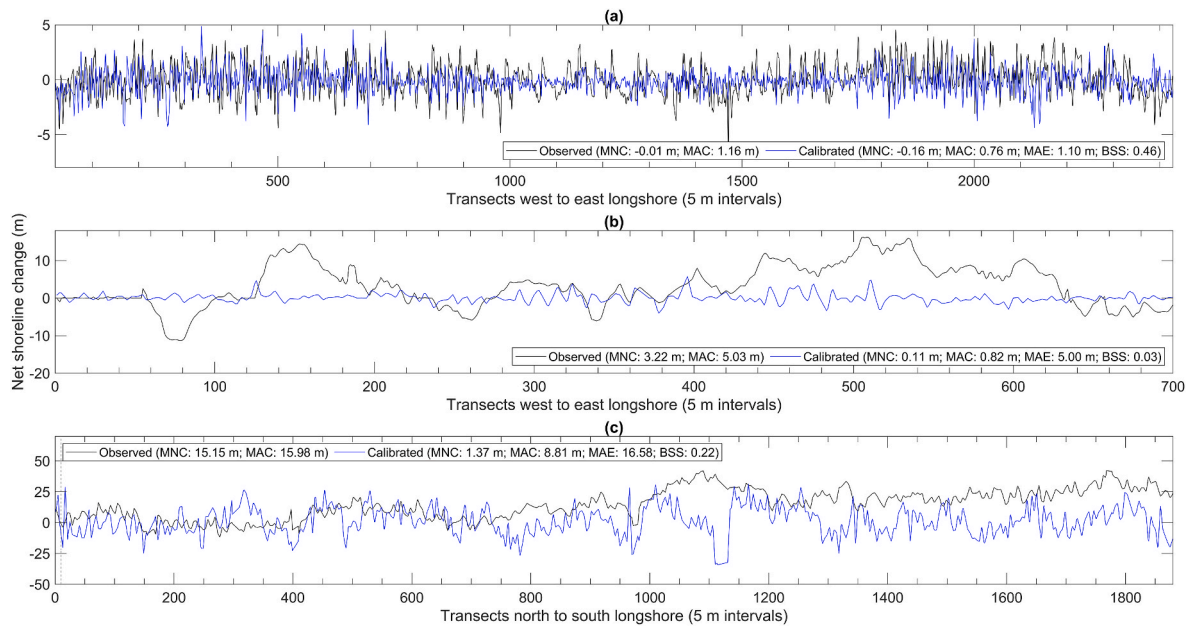


Fig. 15. Longshore variations in shoreline evolution observed and calibrated in the New York (2014–2016) (a), Puerto Rico (2014–2016) (b), and Southern California (2009–2011) (c) test site. MNC is mean net change, MAC is mean absolute change, MAE is mean absolute error, and BSS is Brier Skill score. Note the differences in axes.

The irregular spatial distribution of reef substrate also means that depth contours in reef areas are often not shore-parallel. As the hybrid 2D/one-line approach assumes shore-parallel contours in the morphology update, specifying a closure depth deeper than 5.5 m would have caused errors in shoreline continuity solutions. Shoreline continuity errors occur in these models when depth contours are not shore-parallel because multiple shore-perpendicular coordinates share a common shore-parallel coordinate. Hence, there was no better alternative than specifying a 5.5 m closure depth in PR. The calibrated shoreline evolution predictions presented here, therefore, represent the best outcomes we can get from applying the hybrid 2D/one-line approach at PR.

- (c) Following calibration, shoreline evolution observations and predictions in SC tend to converge in the north but differ in trend component towards the south (Fig. 15c). In the southern part of this site, temporary sand berms are built yearly for protection against winter storms (Fig. 4b) (Gallien et al., 2015). Shoreline evolution observations at this site show net accretion towards the south in line with the annual creation of these berms. The creation of the berms means that the berm height changes annually in the southern part of SC, violating the one-line theory assumption of a fixed berm height that underpins the shoreline morphology update in hybrid 2D/one-line models. As a result, it is perhaps no surprise that the hybrid 2D/one-line approach cannot predict the accretion levels associated with the annual berms in the south (Fig. 15c). Despite this, the hybrid 2D/one-line approach still predicts (i) net accretion (MNC = 1.37 m) in line with the observed trend (MNC = 15.15 m) and (ii) a fluctuating pattern of accretion (mostly) and erosion similar to the fluctuating pattern of accretion magnitudes observed towards the south (Fig. 15c). It is, therefore, likely that the hybrid 2D/one-line approach may be able to better predict shoreline evolution at this location and in more complex planform morphologies if developed to handle temporal and spatial variations in the active coastal profile.

It appears from the calibration results that the hybrid 2D/one-line approach is limited to areas that conform to the one-line theory assumptions of (a) shore-parallel contours and (b) spatially invariable

active coastal profile. The one-line theory underpins the shoreline continuity equation in hybrid 2D/one-line models, such as MIKE21. As NY morphology conforms to the one-line theory assumptions, it is no surprise that MIKE21 performs best in this location. In slight contrast, SC morphology partially conforms to the one-line theory assumptions, which plausibly explains the borderline good performance from MIKE21 at this site. Although SC has shore-parallel contours and a spatially invariable closure depth, it has a temporally and spatially variable beach berm elevation, which defines the landward limit of the active coastal profile. PR morphology does not conform to the one-line theory assumptions, which can explain the corresponding bad performance from MIKE21. PR has a complex planform morphology, characterised by non-parallel depth contours and a spatially variable closure depth..

5. Discussion

5.1. Importance of nearshore spatial discretisation

There are two wider implications of the nearshore discretisation sensitivity results. *First*, the finest nearshore spatial discretisation does not guarantee the most accurate shoreline evolution predictions (Fig. 13; Table 11) as often assumed in related literature (Millar et al., 2007; Williams and Esteves, 2017; Bloemendaal et al., 2018). Although the sensitivity results presented in this paper provide no definite reason for this finding, potential causes include the mesh growth rate (defined as the change in resolution from one element in the mesh to another) and its aspect ratio (defined as the ratio of the longest to the shortest face of a mesh element). Abrupt changes in the size of mesh elements as a result of mesh growth rate and aspect ratio can cause:

- (a) excessively large fluxes to propagate from very coarse elements (e.g. in the offshore zone) to very fine elements (e.g. in the nearshore zone), forcing solutions to diverge and inducing numerical instability. Sudden changes in mesh discretisation in coupled wave, flow and sediment transport models, for example, can erroneously distort wave propagation and reflection properties, causing unreliable calculations of littoral drift (c.f. Qian et al., 1999).

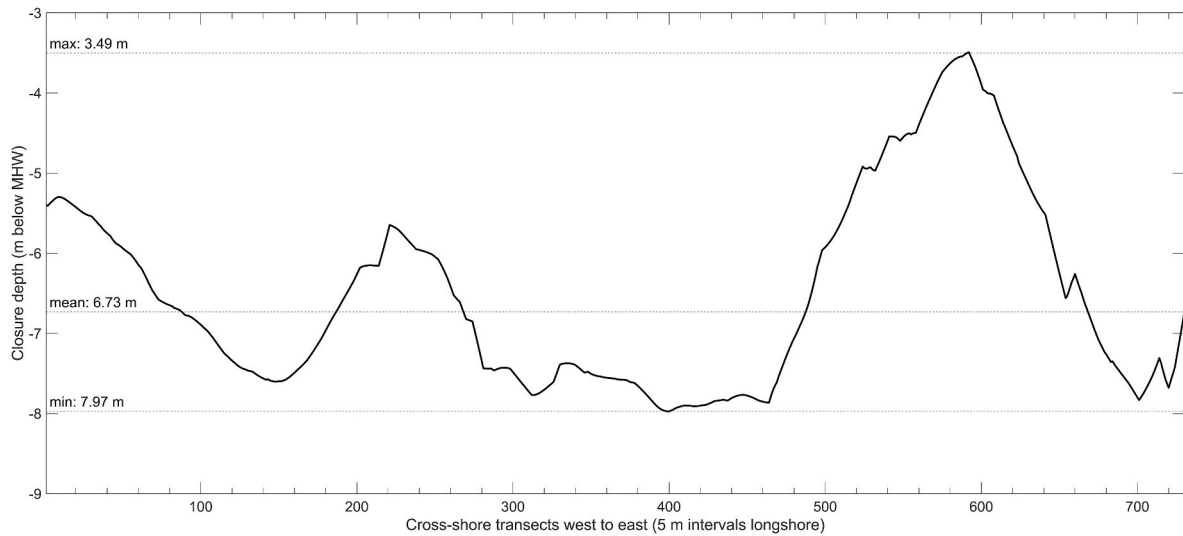


Fig. 16. Closure depth variations in the Puerto Rico test site. In coral reef environments, the first occurrence of reef substrate is considered to be the closure depth.

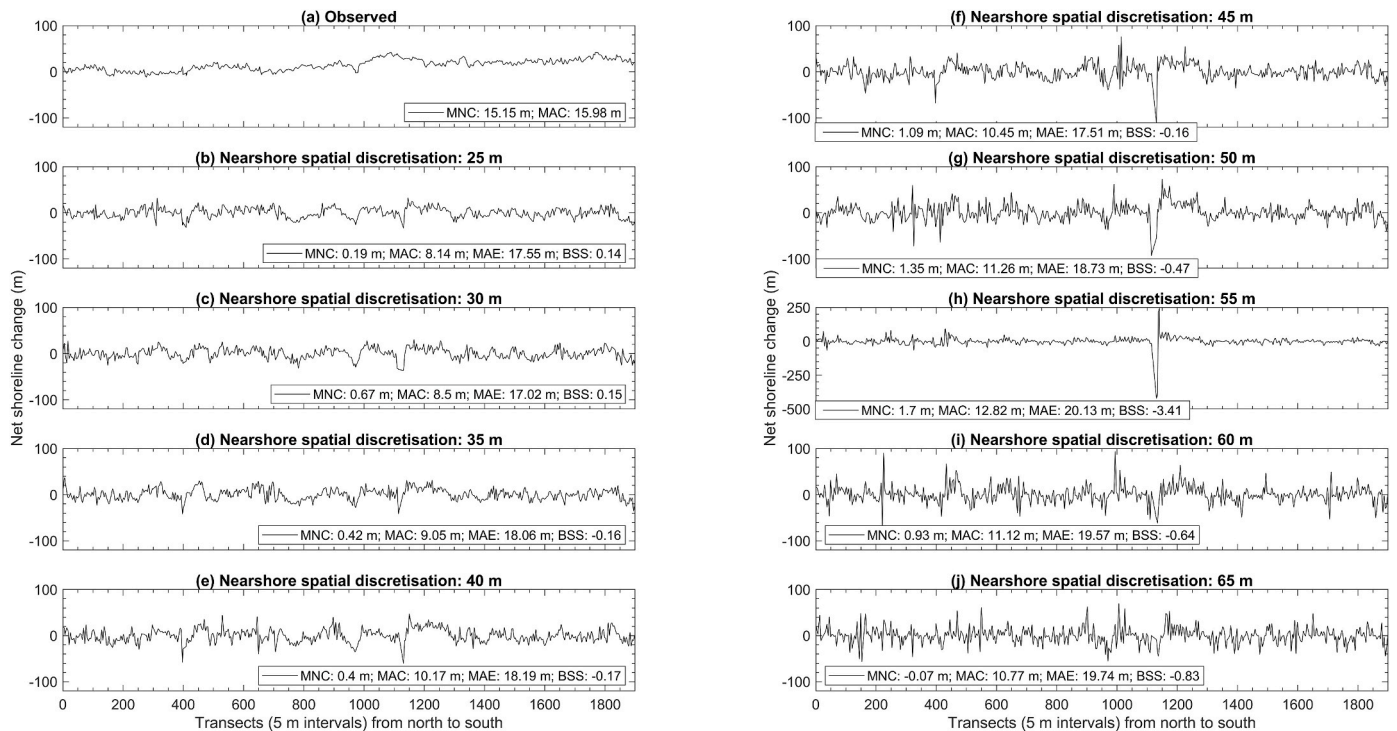


Fig. 17. Shoreline change observed and predicted (2009–2011) in response to coarsening nearshore spatial discretisation in the Southern California test site. MNC is mean net change, MAC is mean absolute change, MAE is mean absolute error, and BSS is Brier Skill Score. Note the difference in y axis in (h).

- (b) truncation errors to accumulate in critical regions with high flow gradients (e.g. regions with high shear), which can destabilise the numerical solution (You et al., 2006). Truncation errors are the difference between the discrete and continuous governing equations. These errors usually contain the diffusive terms (second-order derivatives) where the discretisation applied to such derivatives requires smooth changes between element sizes in the mesh (Jeng and Chen, 1992; Tu et al., 2018).
- (c) numerical instabilities to generate at the open boundaries and propagate inside the domain when the resolution of the boundary conditions specified is not in equilibrium with the variations in resolution between mesh elements (Jones and Davies, 2005; Düben and Korn, 2014).

- (d) considerable mesh skewness, which can cause numerical instability and unreliable predictions (Fabritius and Tabor, 2015; Nishikawa, 2020). For example, MIKE21 process-driven modules are applied using a cell-centred finite volume approach. As a result, the governing equations of these modules are discretised using the distance between the centroids of adjacent mesh elements with the assumption that the vector joining these centroids is normal to the common face. When this assumption is not met, the calculated flux accuracy at the common face reduces as its interpolated value lies at the intersection of the vector joining it to the element centroids. Flux errors at the common face of adjacent elements can prevent model convergence.

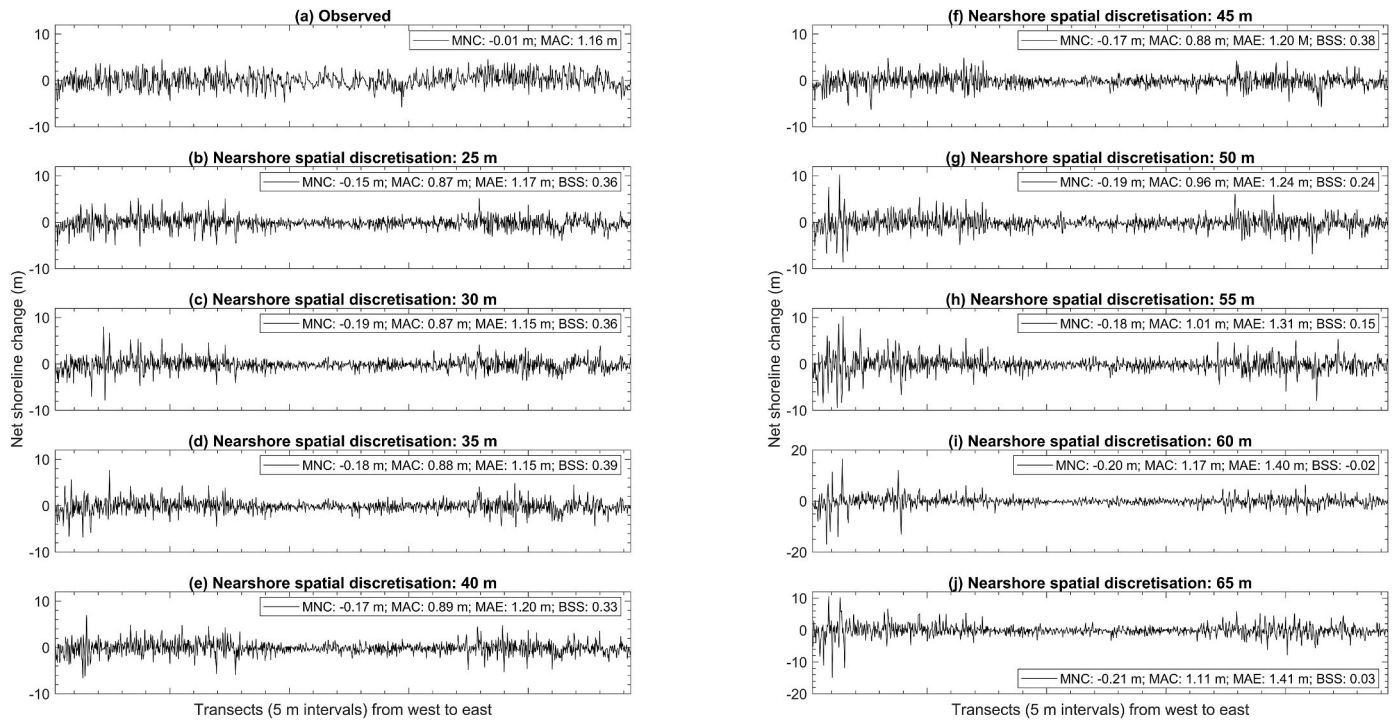


Fig. 18. Shoreline change observed and predicted (2014–2016) in response to coarsening nearshore spatial discretisation in the New York test site. MNC is mean net change, MAC is mean absolute change, MAE is mean absolute error, and BSS is Brier Skill Score. Note the difference in y axis in (i) and (j).

A maximum resolution of 70 m is maintained offshore in all meshes generated whereas the nearshore resolution is varied from 25 to 65 m to assess model sensitivity. The finest nearshore discretisations used are, therefore, associated with the meshes having the largest growth rate and aspect ratio (and hence the most skewness), which may explain why these discretisations are not always associated with the highest shoreline evolution prediction accuracy (Fig. 13; Table 11).

The *second* implication of the nearshore discretisation sensitivity results is that defining a nearshore discretisation based on process length scales does not guarantee reliable shoreline evolution predictions as also assumed in related literature. This insight is analogous to the findings of Hardy et al. (1999). The range of nearshore discretisations used to evaluate model sensitivity in each test site (25–65 m) corresponds to process length scales of primary drivers of shoreline evolution (Table 1). Despite this, nearshore discretisations beyond 30 and 45 m caused a decline in the accuracy of shoreline evolution predictions in SC and NY, respectively (Fig. 13; 17; 18). Along with the DEM used for mesh interpolation, the nearshore discretisation determines how well the observed bathymetry gradients are represented in the model. Errors accumulate in coupled wave, flow, and sediment transport simulations if bathymetry gradients are not in equilibrium with the primary drivers of shoreline evolution forced in the model (cf. Bloemendaal et al., 2018; Bilskie et al., 2020). Therefore, the most reliable nearshore discretisation for simulating shoreline evolution is based on observed coastal system morphology rather than process length scales of shoreline evolution drivers, which is evident from the model sensitivity results. For instance, NY and PR both have a coarser optimal nearshore discretisation than SC even though the range of nearshore discretisations used are fine in spatial resolution relative to the spatial scales over which primary drivers of shoreline evolution operate. As mentioned earlier, this finding correlates with SC having a steeper coastal profile than NY and PR.

The sensitivity results discussed here indicate that nearshore discretisation (including mesh generation criteria) is as important as a typical calibration parameter because (a) it can significantly affect shoreline evolution predictions, which are often used to inform coastal management; (b) it is difficult to determine an optimal nearshore

discretisation *a priori*; and (c) selecting a nearshore discretisation based on the best knowledge of process length scales does not guarantee reliable shoreline evolution predictions.

5.2. Importance of DEM resolution

Together with the nearshore discretisation, the spatial resolution of the DEM used for mesh interpolation determines how well the bathymetry gradients are represented in shoreline evolution models. The bathymetry gradients affect wave-current interactions, which influence the littoral drift gradients that drive shoreline evolution. Related studies use either DEMs that are available without considering the effects on model predictions (Giardino et al., 2018; Le Cozannet et al., 2019; Parodi et al., 2020) or assume the highest DEM resolution produce the most accurate predictions (Splinter et al., 2013; Williams and Esteves, 2017). Contrary to these practices and assumptions, model sensitivity results in each test site show a decline in the accuracy of shoreline evolution predictions as the DEM used for mesh interpolation coarsens beyond a specific resolution, depending on the underlying morphology. In particular, there is a coarser optimal DEM resolution range for mesh interpolation in NY and PR than in SC because of their gentler sloping coastal profile morphology (Fig. 13; Table 12). Steeper coastal profiles degenerate over a smaller range of DEM resolution than gentler profiles (Fig. 14). The degeneration of coastal profiles from coarser DEMs can erroneously distort wave propagation and energy dissipation, which can generate littoral drift gradients that are not in equilibrium with observed coastal morphology (Roelvink et al., 2016). Two inferences can be drawn from the model sensitivity results discussed here. *First*, the optimal DEM resolution depends on coastal profile morphology. *Second*, a high DEM resolution is not always needed to obtain reliable shoreline evolution predictions. This second inference may be limited to simple planform morphologies.

5.3. Relevance of calibrating free parameters

Model sensitivity results indicate that free parameters in shoreline

evolution models do not have standard values that are optimal across all coastal system morphologies. Instead, we can see that the optimal or most accurate values of free parameters depend on coastal system characteristics, as discussed in Section 4. Apart from Manning's n and related friction parameters (e.g. Chezy number), there is a tendency in related literature to accept model default values of free parameters that broadly characterise coastal systems. For example, related studies tend to accept default values of sediment porosity without considering the effects on corresponding predictions (c.f. Drønen et al., 2011; Kristensen et al., 2013; Hendriyono et al., 2015). However, model sensitivity results show a linear relationship between declining model accuracy and increasing sand porosities in NY and PR (Fig. 13d). In contrast, shoreline evolution prediction accuracy in SC increases as sand porosity increases from 0.3 to 0.5 and then declines as sand porosity increases to 0.7 (Fig. 13d). Therefore, while default values of free parameters may fall within an associated range of physically realistic values, it does not mean that these values will be optimal or appropriate for modelling applications across all coastal system morphologies. In some cases, the default values of free parameters in shoreline evolution models can cause significant overprediction or underprediction of shoreline evolution, especially when these values are not in equilibrium with observed coastal morphology and processes (Table 10; Fig. 13). We should, thus, pay greater attention to observed coastal system characteristics than to established physically realistic ranges of free parameters when parameterising shoreline evolution models.

5.4. Hybrid 2D/one-line models

Results indicate that the hybrid 2D/one-line modelling approach may be limited to simple planform morphologies with a stable active coastal profile as in NY (Fig. 2; 15). This limitation is plausibly attributed to the use of the one-line theory for the shoreline morphology update in these models. This attribution stems from the accuracy of calibrated shoreline evolution predictions declining from good in NY ($BSS = 0.5$), to borderline good in SC ($BSS = 0.2$) and bad in PR ($BSS = 0.0$). The morphological assumptions of the one-line theory fully and partially characterises the morphology in NY and SC, respectively. In contrast, the morphology in PR does not conform to the one-line theory assumptions.

The one-line theory assumes shore-parallel depth contours, therefore (a) the shore-normal movement of one contour line is considered a proxy of overall coastal change, and (b) the vertical limits of the active coastal profile are considered constant longshore (Pelnard-Considere, 1956). In complex planform morphologies, such as in PR, wave transformation over non-parallel contours causes spatial variations in wave heights approaching the shoreline, which result in some areas having a shallower closure depth than others (Sabatier et al., 2004; Keshtpoor et al., 2015). Consequently, hybrid 2D/one-line models may fail to simulate the longshore variations in shoreline evolution in these morphologies, which is evident from the calibrated shoreline evolution predictions in PR (Fig. 15b). This limitation corresponds to the closure depth controlling the cross-shore extent of littoral drift distribution in hybrid 2D/one-line models (Kaergaard and Fredsoe, 2013; Kristensen et al., 2013). In complex planform morphologies, the one-line theory assumption of a spatially invariant closure depth in these models can exaggerate or erroneously minimise the cross-shore width of the active coastal profile along several coastal segments longshore (Eversole and Fletcher, 2003). Overestimating the closure depth, for example, pushes the actual seaward extent of the active coastal profile further offshore, which forces littoral drift distribution in areas that will normally be morphologically inactive (Kristensen, 2013). Closure depth overestimations may, therefore, erroneously reduce the volume of littoral drift that will otherwise be distributed inshore, which can cause an over- (under-) prediction of shoreline erosion (accretion) (De Figueiredo et al., 2020). A 5.5 m closure depth was specified in PR, which may explain the bad BSS estimated from the ensuing shoreline evolution predictions since 5.5 m grossly generalises the longshore variability of the closure

depth at this site (Fig. 16).

Underestimating or overestimating the berm elevation can also affect shoreline evolution predictions in a similar way as underestimating or overestimating the closure depth since the berm elevation also (a) determines the cross-shore width of the active coastal profile and (b) influences the cross-shore extent over which littoral drift is distributed. It is, therefore, perhaps no surprise that the accuracy of the hybrid 2D/one-line approach is lower in SC than in NY even though both test sites have simple planform morphologies with shore-parallel depth contours. In SC, the beach berm elevation changes longshore every year in response to the temporary sand berms used for coastal management (Gallien et al., 2015).

Considering the above arguments, allowing the closure depth and beach berm elevation to vary longshore in hybrid 2D/one-line models may enable us to reliably extend these models beyond simple planform morphologies. However, further research is needed to verify this, particularly since the hybrid 2D/one-line modelling approach is becoming increasingly developed and applied over meso timescales with the intent of guiding coastal management (c.f. Ashton and Murray, 2006; Kaergaard and Fredsoe, 2013; Barkwith et al., 2014; Van Maanen et al., 2016; Roelvink et al., 2020).

6. Conclusions

Hybrid 2D/one-line shoreline evolution models are becoming increasingly applied over meso timescales (10^1 – 10^2 years) to inform the management of sandy coastal systems. However, little is known about the key boundary conditions and coastal environmental settings that are needed to effectively apply these models. Therefore, this study assessed (a) the sensitivity of the hybrid 2D/one-line modelling approach, applied through MIKE21, to key boundary conditions in three different sandy coastal system morphologies; and (b) the validity and applicability of this approach in and beyond simple planform morphologies. The most significant findings derived from this study are summarised below:

- The optimal boundary conditions for simulating shoreline evolution are linked to observed coastal system morphology and processes.
- Specifying boundary conditions beyond their optimal range, even if specifications fall within physically realistic ranges, can generate considerable errors in shoreline evolution predictions.
- The nearshore spatial discretisation, which defines the mesh resolution in the nearshore, should be treated as a typical calibration parameter since (i) the finest discretisation does not guarantee the most accurate predictions, and (ii) specifying a discretisation based on the spatial scales over which primary drivers of shoreline evolution operate also does not guarantee reliable predictions.
- The hybrid 2D/one-line modelling approach is not valid for application in complex planform morphologies, defined herein as coastal systems with non-parallel depth contours (e.g. coral reef environments).
- The hybrid 2D/one-line modelling approach have limited applicability in simple planform morphologies, defined herein as coastal systems with shore-parallel contours, where the active coastal profile is subject to direct human modification (e.g. creation of temporary sand berms).
- The hybrid 2d/one-line modelling approach, in its present form, is restricted to simple planform morphologies that conform to the morphological assumptions of the one-line theory.

Findings (d) – (f) are plausibly attributed to the use of the one-line theory, which assumes the active coastal profile maintains a constant time-averaged form and vertical limits (berm height and closure depth), that underpin the shoreline morphology update in hybrid 2D/one-line

models. Allowing the vertical limits of the active coastal profile to vary temporally and spatially may enable the application of the hybrid 2D/one-line modelling approach beyond simple planform morphologies.

CRedit authorship contribution statement

Avidesh Seenath: Conceptualization, Methodology, Validation, Formal analysis, Data curation, Writing – Original, Writing – review & editing, Visualization.

Declaration of competing interest

The authors declare that they have no known competing financial interests or personal relationships that could have appeared to influence the work reported in this paper.

Acknowledgements

Sincerest thanks to Laura Turnbull (Durham University), Richard Hardy (Durham University), and Ian Shennan (Durham University) for providing useful suggestions on various aspects of this study. Earlier versions of this paper were presented at the Coastal Zone Canada 2018 Conference, ECSA 57, DHI Ireland 2018 Symposium, and the 2019 UK Young Coastal Scientists and Engineers Conference. The comments received from the participants at these events and the two anonymous reviewers have been helpful in refining the paper. I am grateful to DHI Water Environments UK Ltd for providing access to MIKE21 (2016–2020) and Mark Bailes for his technical support and assistance with the software.

References

- Ashton, A.D., Murray, A.B., 2006. High-angle wave instability and emergent shoreline shapes: 1. Modeling of sand waves, flying spits, and capes. *J. Geophys. Res.: Earth Surf.* 111, F04011.
- Barkwith, A., Thomas, C.W., Limber, P.W., Ellis, M.A., Murray, A.B., 2014. Coastal vulnerability of a pinned, soft-cliff coastline Part I: assessing the natural sensitivity to wave climate. *Earth Surf. Dyn.* 2, 295–308.
- Bilskie, M.V., Hagen, S.C., Medeiros, S.C., 2020. Unstructured finite element mesh decimation for real-time hurricane storm surge forecasting. *Coast Eng.* 156, 103622.
- Bloemendaal, N., Muis, S., Haarsma, R.J., Verlaan, M., Maaijen, I.A., De Moel, H., Ward, P.J., Aerts, J.C.J.H., 2018. Global modeling of tropical cyclone storm surges using high-resolution forecasts. *Clim. Dynam.* 52, 5031–5044.
- Brunn, P., 1962. sea-level rise as a cause of shore erosion. *J. Waterw. Harb. Div.* 88, 117–130.
- Cattaneo, A., Steel, R.J., 2003. Transgressive deposits: a review of their variability. *Earth Sci. Rev.* 62, 187–228.
- Chow, V.T., 1959. *Open-Channel Hydraulics*. McGraw-Hill, New York.
- Cooper, J.A.G., Masselink, G., Coco, G., Short, A.D., Castelle, B., Rogers, B., Anthony, E., Green, A.N., Kelley, J.T., Pilkey, O.H., Jackson, D.W.T., 2020. Sandy beaches can survive sea-level rise. *Nat. Clim. Change* 10, 993–995.
- Cooper, J.A.G., Pilkey, O.H., 2004. sea-level rise and shoreline retreat: time to abandon the Bruun rule. *Global Planet. Change* 43, 157–171.
- De Figueiredo, S.A., Goulart, E.S., Calliari, L.J., 2020. Effects of closure depth changes on coastal response to sea level rise: insights from model experiments in southern Brazil. *Geomorphology* 351, 106935.
- De Vriend, H.J., Capobianco, M., Chesser, T., De Swart, H.E., Latteux, B., Stive, M.J.F., 1993. Approaches to long-term modelling of coastal morphology: a review. *Coast Eng.* 21, 225–269.
- DHI, 2017. *MIKE 21 Documentation* [Online]. Available: https://manuals.mikepowere.com/dbydhi/help/2017/MIKE_21.htm. January 01 2017.
- Drønen, N., Kristensen, S.E., Taaning, M., Elfrink, B., Deigaard, R., 2011. Long term modelling of shoreline response to coastal structures. In: Wang, P., Rosati, J.D., Roberts, T.M. (Eds.), *The Proceedings of the Coastal Sediments 2011*. World Scientific, Singapore.
- Düben, P.D., Korn, P., 2014. Atmosphere and ocean modeling on grids of variable resolution—a 2D case study. *Mon. Weather Rev.* 142, 1997–2017.
- Eversole, D., Fletcher, C.H., 2003. Longshore sediment transport rates on a reef-fronted beach: field data and empirical models kaanapali beach, Hawaii. *J. Coast Res.* 19, 649–663.
- Fabritius, B., Tabor, G., 2015. Improving the quality of finite volume meshes through genetic optimisation. *Eng. Comput.* 32, 425–440.
- Farnsworth, K.L., Warrick, J.A., 2007. Sources, Dispersal, and Fate of Fine Sediment Supplied to Coastal California. U.S. Geological Survey, Reston, Virginia.
- Folk, R.L., Ward, W.C., 1957. Brazos river bar [Texas]: a study in the significance of grain size parameters. *J. Sediment. Res.* 27, 3–26.
- Franz, G., Delpy, M.T., Brito, D., Pinto, L., Leitão, P., Neves, R., 2017. Modelling of sediment transport and morphological evolution under the combined action of waves and currents. *Ocean Sci.* 13, 673–690.
- Fringer, O.B., Dawson, C.N., He, R., Ralston, D.K., Zhang, Y.J., 2019. The future of coastal and estuarine modeling: findings from a workshop. *Ocean Model.* 143, 101458.
- Gallien, T.W., O'reilly, W.C., Flick, R.E., Guza, R.T., 2015. Geometric properties of anthropogenic flood control berms on southern California beaches. *Ocean Coast Manag.* 105, 35–47.
- Giardino, A., Nederhoff, K., Voudoukas, M., 2018. Coastal hazard risk assessment for small islands: assessing the impact of climate change and disaster reduction measures on ebebe (Marshall Islands). *Reg. Environ. Change* 18, 2237–2248.
- Hanson, H., Aarninkhof, S., Capobianco, M., Jimenez, J.A., Larson, M., Nicholls, R.J., Plant, N.G., Southgate, H.N., Steetzel, H.J., Stive, M.J.F., De Vriend, H.J., 2003. Modelling of coastal evolution on yearly to decadal time scales. *J. Coast Res.* 19, 790–811.
- Hardy, R.J., Bates, P.D., Anderson, M.G., 1999. The importance of spatial resolution in hydraulic models for floodplain environments. *J. Hydrol.* 216, 124–136.
- Hendriyono, W., Wibowo, M., Hakim, B.A., Istiyanto, D.C., 2015. Modeling of sediment transport affecting the coastline changes due to infrastructures in batang - central java. *Procedia Earth. Planet. Sci.* 14, 166–178.
- Horton, R.E., 1906. Weir Experiments, Coefficients, and Formulas. *Series M, General Hydrographic Investigations*. United States Geological Survey, Washington.
- Hurst, M.D., Barkwith, A., Ellis, M.A., Thomas, C.W., Murray, A.B., 2015. Exploring the sensitivities of crenulate bay shorelines to wave climates using a New vector-based one-line model. *J. Geophys. Res.: Earth Surf.* 120, 2586–2608.
- Jeng, Y.N., Chen, J.L., 1992. Truncation error analysis of the finite volume method for a model steady convective equation. *J. Comput. Phys.* 100, 64–76.
- Jones, J.E., Davies, A.M., 2005. An intercomparison between finite difference and finite element (TELEMAC) approaches to modelling West Coast of Britain tides. *Ocean Dynam.* 55, 178–198.
- Kaergaard, K., Fredsoe, J., 2013. A numerical shoreline model for shorelines with large curvature. *Coast Eng.* 74, 19–32.
- Kaye, C.A., 1959. *Coastal Geology of Puerto Rico: Geology of the San Juan Metropolitan Area*. Government Printing Office, Puerto Rico, Washington, D.C., U.S.
- Keshtpoor, M., Puleo, J.A., Shi, F., Dicosmo, N.R., 2015. Numerical simulation of nearshore hydrodynamics and sediment transport down-drift of a tidal inlet. *J. Waterw. Port. Coast. Ocean Eng.* 141, 04014035.
- Kraus, N.C., Larson, M., Wise, R.A., 1998. Depth of Closure in Beach-Fill Design. Coastal Engineering Technical Note. U.S. Army Engineer Waterways Experiment Station, Vicksburg, MS.
- Kristensen, S.E., 2013. Marine and Coastal Morphology: Medium Term and Long-Term Area Modelling. Ph.D. Thesis. Technical University of Denmark.
- Kristensen, S.E., Drønen, N., Deigaard, R., Fredsoe, J., 2013. Hybrid morphological modelling of shoreline response to a detached breakwater. *Coast Eng.* 71, 13–27.
- Le Cozannet, G., Bulteau, T., Castelle, B., Ranasinghe, R., Woppele, G., Rohmer, J., Bernon, N., Idier, D., Louisor, J., Salas, Y.M.D., 2019. Quantifying uncertainties of sandy shoreline change projections as sea level rises. *Sci. Rep.* 9, 42.
- Manson, G.K., 2012. Configuration of Mike21 for the Simulation of Nearshore Storm Waves, Currents and Sediment Transport: Brackley Bight, Prince Edward Island. Geological Survey of Canada, Canada.
- Mattocks, C., Forbes, C., 2008. A real-time, event-triggered storm surge forecasting system for the state of North Carolina. *Ocean Model.* 25, 95–119.
- Millar, D.L., Smith, H.C.M., Reeve, D.E., 2007. Modelling analysis of the sensitivity of shoreline change to a wave farm. *Ocean Eng.* 34, 884–901.
- Mycoo, M., Donovan, M.G., 2017. A Blue Urban Agenda: Adapting to Climate Change in the Coastal Cities of Caribbean and Pacific Small Island Developing States. Inter-American Development Bank.
- NCEI, 2017a. NCEI hurricane sandy digital elevation models [Online]. Available: http://www.ngdc.noaa.gov/mgg/inundation/sandy/sandy_geoc.html, 03 March 2017.
- NCEI, 2017b. *Santa Monica, California 1/3 arc-second NAVD 88 coastal digital elevation model* [online]. Available: <https://data.noaa.gov/metaview/page?xml=NOAA/NESDIS/NGDC/MGG/DEM/iso/xml/726.xml&view=getDataView&header=none#>, 03 March 2017.
- NCEI, 2019. *Santa Monica, Puerto Rico 1/9 arc-second PRVD coastal digital elevation model* [online]. Available: <https://www.ncei.noaa.gov/metadata/geoportal/rest/metadata/item/gov.noaa.ngdc.mgg.dem:11510/html>. June 01 2019.
- NDBC, 2017a. *NDBC - station 44065 recent data* [online]. Available: https://www.ndbc.noaa.gov/station_page.php?station=44065, 01 January 2017.
- NDBC, 2017b. *NDBC - station 41053 recent data* [online]. Available: https://www.ndbc.noaa.gov/station_page.php?station=41053, 01 January 2017.
- NDBC, 2017c. *NDBC - station 46221 recent data* [online]. Available: https://www.ndbc.noaa.gov/station_page.php?station=46221, 03 March 2017.
- Nicholls, R.J., Larson, M., Capobianco, M., Birkemeier, W.A., 1999. Depth of closure: improving understanding and prediction. In: Edge, B.L. (Ed.), *Coastal Engineering, 1999 Copenhagen, Denmark*. American Society of Civil Engineers, pp. 2888–2901.
- Nimmo, J.R., 2013. Porosity and Pore Size Distribution. Reference Module in Earth Systems and Environmental Sciences.
- Nishikawa, H., 2020. A face-area-weighted 'centroid' formula for finite-volume method that improves skewness and convergence on triangular grids. *J. Comput. Phys.* 401, 109001.
- NOAA, 2017a. 2009 - 2011 CA coastal conservancy coastal lidar project: *hydro-flattened bare Earth DEM* [online]. Available: https://coast.noaa.gov/htdata/raster2/elevation/California_Lidar_DEM_2009_1131/ca2010_coastal_dem.html, 03 March 2017.

- NOAA, 2017b. 2016 USGS CoNED topobathymetric model (1887 - 2016): *New england* [online]. Available: <https://inport.nmfs.noaa.gov/inport/item/49419/citation>. March 03 2017.
- NOAA, 2017c. *San juan, La puntilla, san juan bay, Pr - station id: 9755371* [online]. Available: <https://tidesandcurrents.noaa.gov/stationhome.html?id=9755371>, 01 January 2017.
- NOAA, 2017d. *Sandy hook, NJ - station id: 8531680* [online]. Available: <https://tidesandcurrents.noaa.gov/stationhome.html?id=8531680>, 17 November 2017.
- NOAA, 2017e. *Santa Monica, CA - station id: 9410840* [online]. Available: <https://tidesandcurrents.noaa.gov/stationhome.html?id=9410840>, 03 March 2017.
- NOAA, 2019. 2016 NOAA NGS topobathy lidar DEM: *Puerto Rico* [online]. Available: https://coast.noaa.gov/htdata/raster2/elevation/NGS_PR_DEM_2016_8462/, 01 June 2019.
- Parodi, M.U., Giardino, A., Van Dongeren, A., Pearson, S.G., Bricker, J.D., Reniers, A.J.H.M., 2020. Uncertainties in coastal flood risk assessments in small island developing states. *Nat. Hazards Earth Syst. Sci.* 20, 2397–2414.
- Payo, A., French, J.R., Sutherland, J., Ellis, A., M., Walkden, M., 2020. Communicating simulation outputs of mesoscale coastal evolution to specialist and non-specialist audiences. *J. Mar. Sci. Eng.* 8, 235.
- Pelnaud-Considere, R., 1956. *Essai De Theorie De L'evolution Des Formes De Rivage En Plages De Sable Et De Galets*. 4th Journees De L'Hydraulique, Les Energies De La Mer, pp. 289–298.
- Pontee, N.I., 2017. Coastal engineering and management. In: Green, D.R., Payne, J.L. (Eds.), *Marine and Coastal Resource Management: Principles and Practice*. Routledge, Oxford, United Kingdom.
- Preston, J., Hurst, M.D., Mudd, S.M., Goodwin, G.C.H., Newton, A.J., Dugmore, A.J., 2018. Sediment accumulation in embayments controlled by bathymetric slope and wave energy: implications for beach formation and persistence. *Earth Surf. Process. Landforms* 43, 2421–2434.
- Pye, K., Blott, S.J., Brown, J., 2017. Advice to Inform Development of Guidance on Marine, Coastal and Estuarine Physical Processes Numerical Modelling Assessments. *NRW Evidence Report*. Natural Resources Wales, Cardiff, UK.
- Qian, J.-H., Giorgi, F., Fox-Rabinovitz, M.S., 1999. Regional stretched grid generation and its application to the near regcm. *J. Geophys. Res. Atmos.* 104, 6501–6513.
- Reeve, D.E., Horrillo-Caraballo, J., Karunaratna, H., Pan, S., 2019. A New perspective on meso-scale shoreline dynamics through data-driven analysis. *Geomorphology* 341, 169–191.
- Roelvink, D., Huisman, B., Elghandour, A., Ghoni, M., Reynolds, J., 2020. Efficient modeling of complex sandy coastal evolution at monthly to century time scales. *Front. Mar. Sci.* 7, 535.
- Roelvink, J.a.D., Walstra, D.-J.R., Van Der Wegen, M., Ranasinghe, R., 2016. Modeling of coastal morphological processes. In: Dhanak, M.R., Xiros, N.I. (Eds.), *Springer Handbook of Ocean Engineering*. Springer, Dordrecht.
- Rölfer, L., Winter, G., Costa, M.M., Celliers, L., 2020. Earth observation and coastal climate services for small islands. *Clim.Serv.* 18, 100168.
- Sabatier, F., Stive Marcel, J.F., Pons, F., 2004. Longshore variation of depth of closure on a micro-tidal wave-dominated coast. In: Smith, J.M. (Ed.), *Coastal Engineering*, 2004 Lisbon, Portugal. World Scientific, Singapore, pp. 2327–2339.
- Seenath, A., 2018. Effects of DEM resolution on modeling coastal flood vulnerability. *Mar. Geodes.* 41, 581–604.
- Seenath, A., 2021. *Modelling Mesoscale Evolution of Managed Sandy Shorelines with Particular Reference to Caribbean Small Islands*. PhD. Durham University.
- Slott, J.M., Murray, A.B., Ashton, A.D., 2010. Large-scale responses of complex-shaped coastlines to local shoreline stabilization and climate change. *J. Geophys. Res.: Earth Surf.* 115, F03033.
- Splinter, K.D., Turner, I.L., Davidson, M.A., 2013. How much data is enough? The importance of morphological sampling interval and duration for calibration of empirical shoreline models. *Coast Eng.* 77, 14–27.
- Stive, M.J.F., Aarninkhof, S.G.J., Hamm, L., Hanson, H., Larson, M., Wijnberg, K.M., Nicholls, R.J., Capobianco, M., 2002. Variability of shore and shoreline evolution. *Coast Eng.* 47, 211–235.
- Sutherland, J., Peet, A.H., Soulsby, R.L., 2004. Evaluating the performance of morphological models. *Coast Eng.* 51, 917–939.
- Terry, R.D., Keesling, S.A., Uchupi, E., 1956. *Submarine Geology of Santa Monica Bay, California*. Allan Hancock Foundation for Scientific Research, University of Southern California.
- Tu, J., Yeoh, G.-H., Liu, C., 2018. *CFD Mesh Generation: A Practical Guideline*. *Computational Fluid Dynamics*. Butterworth-Heinemann, Oxford, United Kingdom.
- USACE, NYSDEC, 2015. *Atlantic Coast of Long Island, Jones Inlet to East Rockaway Inlet, Long Beach Island, New York Coastal Storm Risk Management Project: Hurricane Sandy Limited Reevaluation Report*, ume 1. Long Beach, NY.
- Valiente, N.G., Masselink, G., Scott, T., Conley, D., Mccarroll, R.J., 2019. Role of waves and tides on depth of closure and potential for headland bypassing. *Mar. Geol.* 407, 60–75.
- Van Maanen, B., Nicholls, R.J., French, J.R., Barkwith, A., Bonaldo, D., Burningham, H., Brad Murray, A., Payo, A., Sutherland, J., Thornhill, G., Townend, I.H., Van Der Wegen, M., Walkden, M.J.A., 2016. Simulating mesoscale coastal evolution for decadal coastal management: a New framework integrating multiple, complementary modelling approaches. *Geomorphology* 256, 68–80.
- Wentworth, C.K., 1922. A scale of grade and class terms for clastic sediments. *J. Geol.* 30, 377–392.
- Williams, J.J., Esteves, L.S., 2017. Guidance on setup, calibration, and validation of hydrodynamic, wave, and sediment models for shelf seas and estuaries. *Adv. Civ. Eng.* 2017, 5251902.
- You, D., Mittal, R., Wang, M., Moin, P., 2006. Analysis of stability and accuracy of finite-difference schemes on a skewed mesh. *J. Comput. Phys.* 213, 184–204.